Received: 3 November 2017 | Accepted: 5 April 2018

DOI: 10.1111/fog.12381

ORIGINAL ARTICLE

WILEY FISHERIES OCEANOGRAPHY

Climate variability and sardine recruitment in the California Current: A mechanistic analysis of an ecosystem model

Dimitrios V. Politikos[1] | Enrique N. Curchitser[1] | Kenneth A. Rose[2] | David M. Checkley Jr[3] | Jerome Fiechter[4]

[1]Department of Environmental Sciences, Rutgers University, New Brunswick, New Jersey

[2]Horn Point Laboratory, University of Maryland Center for Environmental Science, Cambridge, Maryland

[3]Scripps Institution of Oceanography, University of California, San Diego, La Jolla, California

[4]Ocean Sciences Department, University of California, Santa Cruz, California

Correspondence
Enrique N. Curchitser, Department of Environmental Sciences, Rutgers University, New Brunswick, NJ 08901.
Email: enrique@marine.rutgers.edu

Abstract

Recruitment varies substantially in small pelagic fish populations. Understanding of the mechanisms linking environment to recruitment is essential for the effective management of fisheries resources. In this study, we used a fully coupled end-to-end ecosystem model to study the effect of climate variability on sardine recruitment in the California Current System during 1965–2006. Ocean variability was represented by ROMS hydrodynamic and NEMURO biogeochemical models, and sardine population dynamics was simulated through a full life cycle individual-based model. Model analysis was designed to elucidate how changes in abiotic and biotic conditions may impact the spawning habitats, early life stage survival, and ultimately recruitment of sardine. Our findings revealed the importance of spatial processes to shape early life stages dynamics. Shifts in spawning habitats were dictated by the spatial variations in temperature and the behavioral movement of adults. Additionally, the spatial match of eggs with warmer temperatures and larvae with their prey influenced their survival. The northward shifts in spawning locations and the accomplishment of good recruitment in warmer years agreed with existing knowledge. Egg production and survival during egg and yolk-sac larval stages were key factors to drive the long-term variations in recruitment. Finally, our analysis provided a quantitative assessment of climate impact on year-to-year variation in sardine recruitment by integrating multiple hypotheses.

KEYWORDS

California Current, climate variability, early life stages, individual-based model, mechanistic understanding, Pacific sardine, recruitment

1 | INTRODUCTION

Stocks of small pelagic fish such as sardine and anchovy support important fisheries in most productive coastal regions around the globe and constitute a major energy pathway from lower to higher trophic levels (Ganias, 2014). One important characteristic of these stocks is their interannual-to-multidecadal fluctuations in abundance, mainly attributed to ocean variability and fishing (Alheit, Roy, & Kifani, 2009; Lluch-Belda et al., 1989). Understanding of the mechanisms causing these fluctuations is necessary for accurate prediction of fish population responses to future climate change (Checkley, Asch, & Rykaczewski, 2017).

In the California Current System (CCS), Pacific sardine has undergone drastic fluctuations in catch, abundance and recruitment over the last century (Hill, Crone, & Zwolinski, 2017; Lindegren, Checkley, Rouyer, MacCall, & Stenseth, 2013). These fluctuations were associated with known modes of climate variability on interdecadal (Pacific Decadal Oscillation, North Pacific Gyre Oscillation) and interannual (El-Niño-Southern Oscillation) time scales (Alheit et al., 2009; Chavez, Ryan, Lluch-Cota, & Niquen, 2003; King, 2005). Differences in

spawning and suitable habitats of Pacific sardine have been correlated with patterns of various physical and biotic conditions, such as eddies (Logerwell, Lavaniegos, & Smith, 2001), equatoward wind forcing (Song et al., 2012), temperature (Bakun & Broad, 2003; Song et al., 2012), chlorophyll (Zwolinski, Emmett, & Demer, 2011), dynamic sea surface height (Asch & Checkley, 2013), and curl-driven upwelling (Rykaczewski & Checkley, 2008). During warmer El Niño years, sardines tend to spawn more to the north and closer to the shore, using habitats that appear more favourable for their feeding and offspring survival (Agostini, Bakun, & Francis, 2007; Hargreaves, Ware, & McFarlane, 1994; MacCall, 2009). Conversely, the spawning areas of sardine appear to broaden to more offshore during colder La Niña years due to increased wind-driven offshore transport (Song et al., 2012). Warming years have also favoured sardine egg production (Song et al., 2012) and led to successful year classes (Bakun & Broad, 2003; Lindegren & Checkley, 2013), despite being characterized by lowered primary productivity (Bakun & Broad, 2003). The overall picture is that the sardine population responds rapidly to environmental changes in the CCS by adopting its spawning behavior and shifting its distribution to occupy habitats good for reproductive success.

Pacific sardine stock assessments have shown that recruitment is highly variable (Hill et al., 2017). Stock-recruitment models have attempted to explain this variability based on statistical correlations. These correlations were inferred from different drivers such as temperature (Lindegren & Checkley, 2013), oceanographic indices (PDO, NPGO and MEI, [Jacobson & MacCall, 1995; Galindo-Cortes, De Anda-Montanez, Arreguin-Sanchez, Salas, & Balart, 2010;]), variations in the spawning stock biomass of sardine and changes in the somatic condition of parents (Zwolinski & Demer, 2013). Despite several explanations, understanding the full array of climate-induced effects on recruitment of Pacific sardine remains a topic of ongoing research.

Characterizing the mechanisms of recruitment success is complex because numerous processes, related to feeding, transport, survival, density dependence, predation, batch fecundity, and spawning frequency, act synergistically on fish life cycle to determine year class strength (Ganias, 2014; Houde, 2008; Pritt, Roseman, & O'Brien, 2014). Biophysical individual-based models (IBMs) are ideal tools for studying how these processes may affect growth, mortality and recruitment in fish populations (Garćia-Garćia, Ruiz-Villarreal, & Bernal, 2016; Kristiansen, Drinkwater, Lough, & Sundby, 2011; Okunishi et al., 2012; Ospina-Alvarez, Catalan, Bernal, Roos, & Palomera, 2015; Siddon et al., 2013; Xu, Chai, Rose, Niquen, & Chavez, 2013). These mechanistic models include species-specific physiological and behavioral characteristics of fishes and explore changes in their early life history, driven by differences in abiotic and biotic conditions. Recently, Rose et al. (2015) developed a fully coupled end-to-end ecosystem model to explore the effects ocean-climate variability on anchovy and sardine in the CCS. Their end-to-end framework combined hydrodynamic, biogeochemical, individual-based, and fishing models, and provided a 50 year (1959–2008) historical simulation that successfully reproduced observed decadal-scale variability in sardine biomass. In a companion paper, Fiechter, Rose, Curchitser, and Hedstrom (2015) identified potential correlations between climate variability and sardine abundance of different stages (egg, age-0, adult) that could explain the observed population cycles.

Using the modeling framework of Rose et al. (2015), our goal here was to explore how spatial and temporal changes in physics and biogeochemistry may drive shifts in sardine habitats, affect egg production and early life stages survival, and ultimately contribute to higher or lower recruitment. Our focus was on identifying spatial and temporal differences in the early life history of sardine, especially between warmer El Niño and colder La Niña years, differed markedly with regard to environmental conditions. In addition, we examined to what extent climate variability was responsible for the long-term and year-to-year variations in sardine recruitment. We conclude by comparing model results to existing knowledge and data and discuss key model uncertainties.

2 | MATERIALS AND METHODS

2.1 | End-to-end ecosystem model

For our analysis, we used the fully coupled end-to-end model configured for anchovy and sardine in the CCS (Rose et al., 2015). The end-to-end framework consists of the ROMS general circulation submodel, the NEMURO nutrient–phytoplankton–zooplankton-detritus (NPZD) submodel, a multispecies fish individual-based submodel (IBM) and an agent-based fishing fleet submodel (Figure 1). The full description of these submodels can be found in Rose et al. (2015). Herein, we provide a summary of the model setup with a focus on sardine.

2.2 | Ocean circulation – NPZD submodels

The CCS ocean circulation dynamics was resolved by implementing the Regional Ocean Modeling System (ROMS; Haidvogel et al., 2008; Shchepetkin & McWilliams, 2005). The ROMS model domain extended from 20 to 50°N and 116 to 140°W, with a horizontal resolution of 1/7° (ca. 10 km) and 42 vertical layers. The NPZD model for the CCS was based on the North Pacific Ecosystem Model for Understanding Regional Oceanography (NEMURO; Kishi et al., 2007), which includes three limiting nutrients (nitrate, ammonium, and silicic acid), two phytoplankton groups (nanophytoplankton and diatoms), three zooplankton groups (small- (ZS), large- (ZL), and predatory (ZP) zooplankton), and three detritus pools (dissolved and particulate organic nitrogen and particulate silica). Water velocity and temperature fields from ROMS, and ZS, ZL, and ZP concentrations from NEMURO provided the physical and biological forcing for the IBM model.

2.3 | IBM-Predation-Fishing fleet submodels

The IBM model represented the full life cycle of sardine by integrating its key life-history processes: growth, mortality, movement and

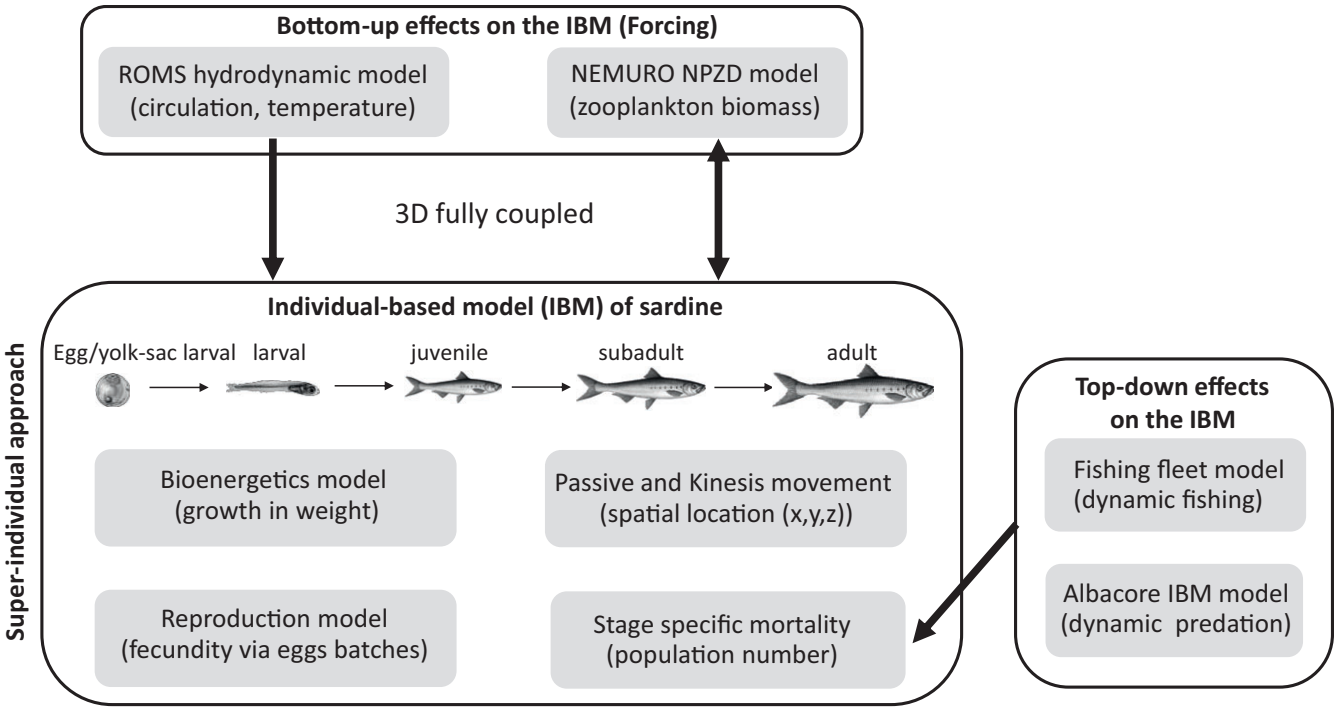

FIGURE 1 Schematic structure of the fully coupled climate-to-fish ecosystem model, showing the coupling of the ROMS, NEMURO NPZD, fish, predation and fishing submodels. The individual-based model of sardine consists of the egg, yolk-sac larval, larval, juvenile, subadult and adult stages

reproduction. The specifics of these processes were described in detail in Rose et al. (2015) and reviewed herein.

2.3.1 | Computational approach

We used a super-individual approach built upon Scheffer, Baveco, DeAngelis, Rose, and van Nes (1995). Each super-individual represented a number of identical individuals, which when summed over all super-individual results in population-level dynamics. The number of identical individuals represented by a super-individual (referred as their worth) was reduced each time step due to mortality, and new super-individuals were introduced through reproduction. When super-individuals reach a maximum age, they are removed, and these super-individuals are used to capture next year's reproduction. The super-individual approach allows for simulation of large-number populations using a fixed number of individuals in the model. All individuals represented by a super-individual shared the same attributes in terms of life stage, age, feeding preferences, mortality rate, worth, location, behavior, and fecundity.

2.3.2 | Life cycle

The life cycle of sardine was divided into six life stages: egg, yolk-sac larval, larval, juvenile, subadult, and adult. Temperature determined the stage duration of eggs and yolk-sac larvae, larvae metamorphosed into juveniles at 35 mm, and juveniles became subadults on 1 January of the next year. The probability of an subadult individual of being a mature adult increased with its length. All individuals were aged by 1 year on 1 January regardless of their actual age in days.

2.3.3 | Growth

A bioenergetics equation computed the growth of sardine as the difference between consumption and respiration rates, with an additional spawning related weight loss term for mature individuals. Maximum fish consumption was weight- and temperature-dependent, and a functional response relationship determined the realized fish consumption rate. The functional response included vulnerability parameters (ranging from 0 meaning not eaten to 1 meaning all prey are available) and feeding efficiency parameters (half-saturation constants) for each life stage on the three zooplankton types (ZS, ZL, PZ) in the NEMURO submodel. No feeding was assumed for sardine eggs and yolk-sac larvae, while larvae and older stages showed full feeding preference on SZ (vulnerability values of 1) and limited preference on LZ and PZ (vulnerabilities: 0.1 and 0.0 for larvae, 0.2 and 0.2 for juveniles, 0.4 and 0.2 for adults, respectively). Fish consumption rates on SZ, LZ and PZ were accumulated over super-individuals and then used as mortality terms in the NEMURO NPZD submodel.

2.3.4 | Mortality

Fixed natural mortality rates were defined for each life stage. Additional mortality, due to starvation, occurred when fish weight dropped below 50% (for larvae) and 40% (for juveniles and adults) of their expected weight calculated from weight-length relationships.

Adult sardines were also subjected to dynamically imposed daily predation and fishing mortalities represented by the predation and fishing fleet submodels.

2.3.5 | Predation and fishing

A migratory predator species (roughly resembling albacore) was used to generate a consumption rate on sardine and then used to impose dynamically-varying predation mortality. The position of each albacore individual in 2-dimensional (horizontal) space was updated hourly using an algorithm that allowed for them to find high prey (e.g., sardine) and all sardines in the water column below the surface cell occupied by each predator individual was assumed to be vulnerable to predation. Like albacore, individual fishing boats were also moved horizontally using the surface layer of the ROMS grid, and they could encounter all sardine individuals in the water column below each surface cell. A trip by a boat was completed within 24 hr, including the time to travel to the cells to fish and the time to return to the nearest port from the last cell fished.

2.3.6 | Movement

Egg, yolk-sac larval and larval stages were considered as passive drifters, so their movement was dictated by ocean circulation. Juvenile and adult stages had the ability to move to specific habitats based on their thermal and feeding preferences. To this end, sardines performed horizontal displacements using the kinesis movement algorithm (Humston, Olson, & Ault, 2004; Watkins & Rose, 2013). Kinesis allowed fish to move and remain close to optimal habitats by weighting inertial and random velocity components, thus allowing behavior to adjust in response to changing environmental conditions. Temperature and zooplankton concentrations were used as cues to determine the behavioral movement of sardines, which was defined by a local search for temperatures close to an optimum, set at 13.5°C, and better feeding conditions. Unfavourable conditions led sardines to perform a more active random search (random component) of the surrounding environment to locate better habitats, whereas when conditions were near optimal fish maintained their current behavior (inertial component). In addition, a northward feeding migration of age-1 and older sardines during summer (June) to feed and their return in the early fall (September) was simulated using kinesis algorithm by changing the probability of north-south movement. Sardines super-individuals initially were randomly placed between 34–46°N, and 120–160 km offshore.

2.3.7 | Reproduction

Potential spawning period lasted from 1 February to 1 July. During a day, actual spawning took place under a set of conditions. Mature anchovies produced new eggs when they experienced temperature at midnight within the range of 12–15°C and had stored the energy required to release a batch. The batch fecundity (number of eggs released per spawning event) depended on fish weight at a rate of 260 eggs/gr-fish and consumption rate. Multiple batches were possible, after imposing a resting time between batches so that individuals could accumulate the energy needed for releasing a new batch.

2.3.8 | Simulation run

The earlier historical simulation reported in in Rose et al. (2015) was repeated here using an extended version of spatial domain (extended southward to 32°N). The new simulation was then analyzed for sardine population dynamics. To agree as best as possible with estimated recruitment, we slightly adjusted the mortality rate for the larval stage to 0.1245/day (0.125/day in Rose et al., 2015) and the initial worth of age-1 super-individuals to 4,000 million (5,000 million in Rose et al., 2015).

2.4 | Model analysis

Our analysis of the historical simulation was designed to elucidate how changes in abiotic (circulation, temperature) and biotic (zooplankton) conditions, simulated by ROMS-NEMURO submodels, can affect the spawning grounds of sardine, induce changes in early life stage survival, and ultimately determine recruitment strength. We also explored related hypotheses concerning habitat shifts and improved reproductive success during warmer years (Agostini et al., 2007), and drivers of good or poor recruitment (Bakun & Broad, 2003). To achieve this, within the historical simulation run, we focused on the effects of warm (1992, 1998, 2003) and cold (1989, 1999, 2002) years. These specific years were chosen because they were associated with known El Niño-Southern Oscillation (ENSO) events in the North Pacific (King, 2005; Murphree & Reynolds, 1995; Song et al., 2012); observations were also available in these years to evaluate model performance.

Temperature and zooplankton concentrations, averaged in sardine locations, were used to quantify variation in environmental conditions and thus avoided the need to average fields over subregions in which sardines were not present. Hovmöller plots (Hocke & Kämpfer, 2011) were used to map the month-to-year evolution of temperature and zooplankton. Changes in spawning activity over time reflect variations in physical conditions and suitable habitats for egg release and survival (Ganias, 2014). To follow spatial shifts in spawning habitats, we calculated the centre of their distribution (longitude, latitude) by averaging over the locations of egg super-individuals and statistically weighting by their worth.

In the IBM, the geographic range of spawning activity was dictated by two factors: the spatial variation of temperature and the behavioral movement of adult sardines during the spawning period. First, temperatures between 12 and 15°C set the allowed limits for mature sardines to release eggs. This implied that spatial shifts in these isotherms may alter potentially the spawning locations. Second, adults adjusted their habitats by searching for prey concentrations that increased their consumption rates and temperatures close to a prescribed optimum, set at T_{opt} = 13.5°C (Rose et al., 2015). To understand the link between shifts in spawning habitats and changes in adult distribution, we considered a habitat index (I_H) for adults

TABLE 1 List of processes examined to understand the linkage of climate variability with sardine recruitment variability and their computation from model outputs

Life stage	Processes	Computation
Egg and yolk-sac larval	Survival	The fraction of each egg super-individual's worth survived to larval stage was recorded for each year. The fractions were then weight-averaged over all egg super-individuals by their worth. By this way, we computed annual egg and yolk-sac larval survival
Egg and yolk-sac larval	Match-mismatch	The abundance of eggs released daily from each mature super-individual for each horizontal grid cell was recorded over the spawning period, as well the temperature experienced by eggs during their release. A bivariate histogram pictured their overlap
Larval	Survival	The fraction of each larval super-individual's worth survived to juvenile stage was recorded for each year. The fractions were then weight-averaged over all larval super-individuals by their worth. By this way, we computed annual larval survival
Larval	Match-mismatch, Dispersal	The abundance of larvae was summed daily over all super-individuals in the water column for each horizontal grid cell. The abundances were then averaged over the year using as weighing factor the daily total abundance. The zooplankton experienced by larvae was also averaged daily using the worth of super-individuals as weighting factor. Daily zooplankton was then averaged over the year. A map showing the overlap of larval abundance with experienced zooplankton was produced for each year
Adult	Total annual egg production	The number of eggs released by each super-individual in every batch was multiplied by the worth of the super-individual at time of each release. Total annual egg production was the sum of the total eggs released over all super-individuals in each year

using two functions: the food function I_{food} and the temperature function I_{temp}. I_{food} quantified the proportion of maximum fish consumption (called p_{value} in bioenergetics literature) by combining ZS, ZL, and ZP zooplankton groups through diet preferences and feeding efficiencies, and ranged between 0 (poor feeding) and 1 (high feeding) (Rose et al., 2015). I_{temp} measured the absolute deviations of temperatures experienced by adult sardines from T_{opt}, as follows:

$$I_{temp} = \frac{|T - T_{opt}|}{\sigma_T},$$

where T is temperature in fish locations, and σ_T (2.0°C) is a tolerance value (i.e., standard deviation, σ_T), defined in the kinesis algorithm. The value of σ_T determines how quickly the inertial component of behavior decreases in influencing movement as temperature deviates from its optimal value. The closer the fish is to T_{opt}, the closer the I_{temp} to zero. Then, a composite habitat index (I_H) was calculated as the geometric mean of I_{food} and I_{temp} following Zajac, Stith, Bowling, Langtimm, and Swain (2015):

$$I_H = \sqrt{I_{food} \times \frac{1}{I_{temp}}}$$

I_H is high in regions where I_{food} is high and I_{temp} is low. I_{food} and I_{temp} were calculated daily for each grid cell, weighted by the worth of mature super-individuals, then averaged from 1 February to 1 July to cover the spawning period, and finally normalized between 0 and 1. The temperatures and food used in the analysis were those experienced by each super-individual (Lagrandian trackers), rather than the values in cells or subregions of the grid. The final results are spatial maps that depicted regions with good forage conditions (I_{food}), temperatures around optimum (I_{temp}), and, ultimately, favourable habitats for adults (I_H).

In our analysis, we also explored the contribution of potential processes as explanatory variables for explaining long-term and year-to-year variability in sardine recruitment (Table 1). Early life stage survival is a primary determinant of recruitment success (Bradford & Cabana, 1997; Ganias, 2014). Herein, the fraction of eggs and yolk-sac larvae that survived to the first feeding larval stage is denoted as egg survivorship, and the fraction of larvae that survived to the juvenile stage is denoted as larval survivorship (Table 1). The "match-mismatch hypothesis" has been proposed as a major mechanism affecting fish recruitment (Cushing, 1974; Houde, 2008). It argues that survival depends on the spatio-temporal overlap of fish with their environment. A match with high overlap can ensure higher growth and survival and contribute to higher recruitment. Conversely, a mismatch can cause low growth and survival and lead to lower recruitment. In addition, fish early-life stages are exposed to the general circulation as passive drifters and their dispersal to unfavourable areas might significantly affect their survival ("Aberrant Drift" hypothesis, [Hjort, 1926]).

To test the match-mismatch hypothesis in our historical simulation, we examined to what extent the spatial overlap of eggs and yolk-sac larvae with temperature and larvae with zooplankton concentrations could affect their survival (Table 1). An estimate of the match-mismatch between fish and environment was obtained by using bivariate histograms. A bivariate histogram is a rectangular array of tiles with colours indicating the bin values. Bivariate histograms were plotted with "histogram2" function in MATLAB software (http://www.mathworks.com). At the population level, variations in annual egg production appear to have a positive correlation with levels of recruitment (Ganias, 2014), although more eggs do not necessarily assure higher recruitment because of the high and variable mortality rates of early life stages (Ganias, 2014; Ospina-Alvarez et al., 2015). In the model, we denoted as annual egg production the sum of eggs produced from all spawners over their multiple batch releases in each year and investigated its contribution to variations in recruitment. Simulated annual recruitment was defined as the sum of worth over all juvenile super-individuals survived at the end of each year.

To assess the contribution of egg production (Egg-Prod), egg and yolk-sac larval survival (EYS-S), and larval survival (Larval-S) to the

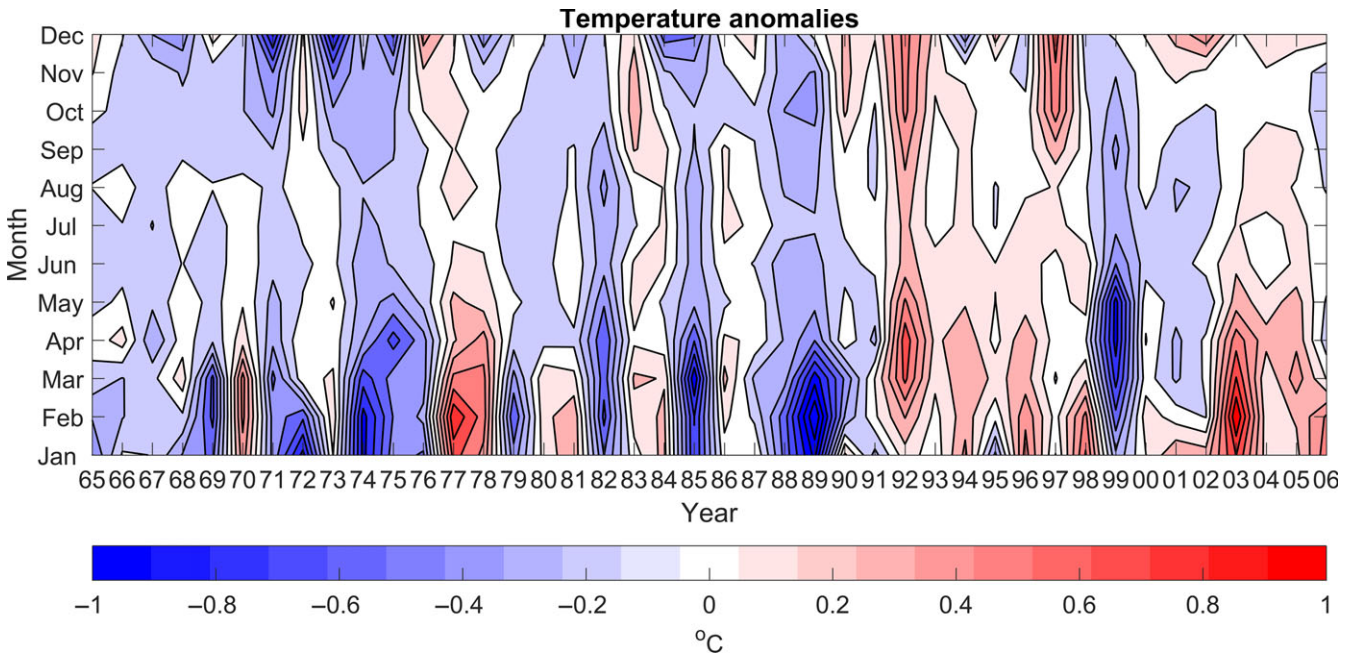

FIGURE 2 Monthly temperature anomalies (*y*-axis) over 1965–2006 (*x*-axis). Hovmöller plot depicted positive temperature anomalies during warmer years (1992, 1998 and 2003), and negative temperature anomalies during colder years (1989, 1999 and 2002). Anomalies were calculated by removing the 1965–2006 mean per month (value-monthly mean). Temperatures were averaged daily over all adult super-individuals, weighted by their worth, and then averaged monthly [Colour figure can be viewed at wileyonlinelibrary.com]

long-term variability in annual recruitment (Rec), we used a multiple regression model:

$$\text{Rec} \sim b_o + b_1 * \text{Egg-Prod} + b_2 * \text{EYS-S} + b_3 * \text{Larval-S} \quad (1)$$

To get standardized regression coefficients, we standardized both explanatory variables (Egg-Prod, EYS-S and Larval-S) and the response variable (Rec) by subtracting the mean from their original value and dividing by their standard deviation. Additionally, to calculate the contribution of explanatory variables in terms of percent, we used the R package "relaimpo" (Groemping, 2010) and specifically the "lmg metric" that measures the R^2 partitioned by averaging over the explanatory predictors (Chevan & Sutherland, 1991).

We were also interested in quantifying how year-to-year variations in explanatory variables (Egg-Prod, EYS-S, Larval-S) affected recruitment (Rec). This was important to assess how fast recruitment was changing interannually (i.e., recruitment change rate) due to the synergistic effect of explanatory variables. For this purpose, we calculated the annual rates of change (ARC),

$$\text{ARC}_y = \left(\frac{V_y - V_{y-1}}{V_y}\right) * 100,$$

where V_y is the value for each explanatory and response variable in year y. Then, we computed the anomalies in annual rates of change (AARC in %) for each predictor and response variable as the difference:

$$\text{AARC}_y = \text{ARC}_y - \overline{\text{ARC}},$$

where $\overline{\text{ARC}} = \frac{\sum_{y=1}^{42} \text{ARC}_y}{42}$ is the average of annual ARC changes over 1965–2006.

Additionally, correlations were computed between temperature and the centre of egg distributions and EYS survival. For larval stage, we calculated correlations between SZ (main prey for larvae) and the centre of larval distributions and survival. Finally, to further evaluate our analysis, we compared aspects of model results to available field data. Simulated sardine recruitment was plotted against estimated recruitment (Hill et al., 2017), and predicted distributions of sardine eggs and larvae were compared with abundance maps of eggs and larvae collected during the California Cooperative Oceanic Fisheries Investigation (CalCOFI) surveys (http://calcofi.org/data.html).

3 | RESULTS

3.1 | Temperature and zooplankton experienced by sardine

Monthly temperature anomalies experienced by sardines showed notable seasonal variations between warm and cold years (Figure 2). Warmer years resulted in positive temperature anomalies on average by: ~0.44°C in 1992, ~0.50°C in the early 1998 and ~0.70°C in 2003. In contrast, the negative temperature anomalies noticed in 1989 (on average by −0.5°C), 1999 (on average by −0.6°C) and 2002 (on average by −0.2°C) aligned with the occurrence of cool waters during La Niña events.

Seasonal variations in total zooplankton biomass (SZ+LZ+PZ) were associated with changes in temperature conditions. The negative zooplankton anomalies mostly prevailed during 1992 (on average by −0.088 mmolN/m^3), 1998 (on average by −0.055 mmolN/

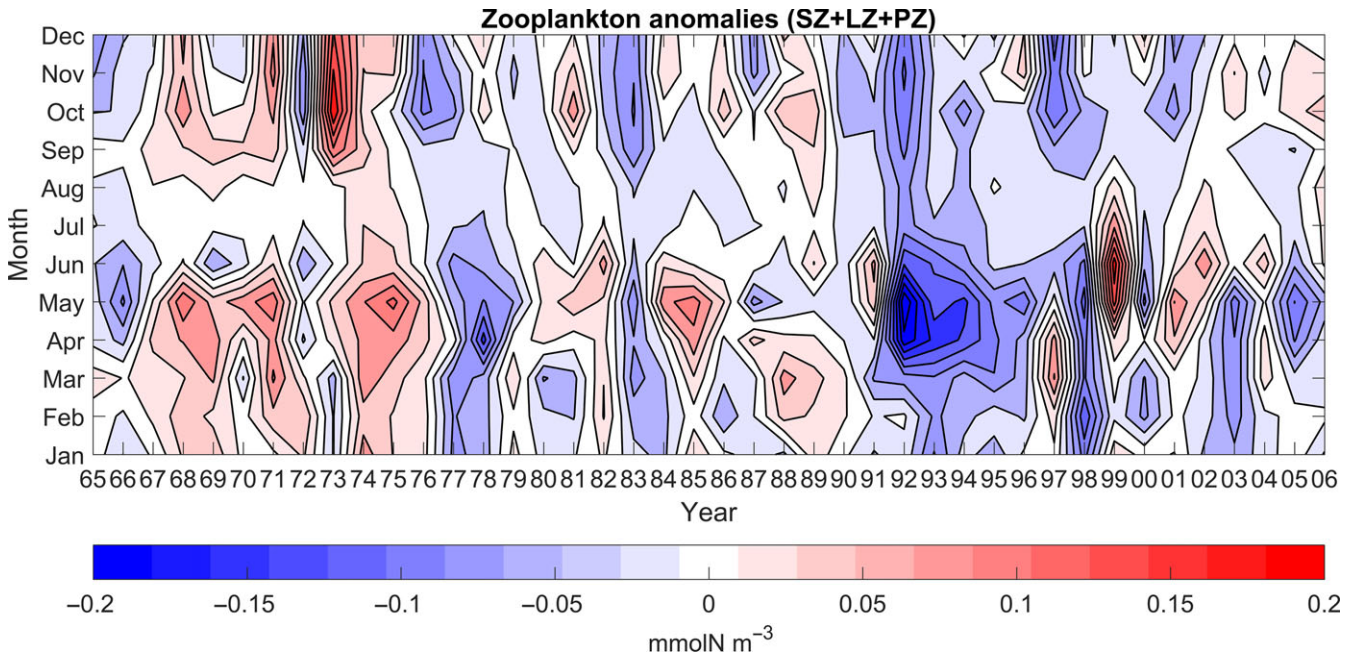

FIGURE 3 Monthly anomalies of total zooplankton (SZ, LZ, PZ) (*y*-axis) over 1965–2006 (*x*-axis). Hovmöller plot depicted negative zooplankton anomalies during warm years (1992, 1998, 2003), and return to neutral and positive zooplankton anomalies during cold years (1989, 1999, 2002). Anomalies were calculated removing the 1965–2006 mean per month (value-monthly mean). Zooplankton concentrations were averaged daily over all adult super-individuals, weighted by their worth, and then averaged monthly [Colour figure can be viewed at wileyonlinelibrary.com]

m^3), and 2003 (on average by −0.019 mmolN/m^3), (Figure 3) were associated with increased temperatures during these years (Figure 2). Conversely, sardined experienced better feeding conditions during colder years, resulting in positive zooplankton anomalies on average by: +0.033 mmolN/m^3 in 1989, +0.038 mmolN/m^3 in 1999 and +0.009 mmolN/m^3 in 2002 (Figure 3).

3.2 | Changes in spawning habitats

The spatial extent of spawning habitats shifted markedly between warm and cold years. During the warming conditions in 1992, 1998, and 2003, spawning activity favoured north of 37°N and deceased south of 34°N (Figure 4). In contrast, during colder years (1989, 1999, and 2002), eggs were mostly located between 32 and 37°N (Figure 4). The shift of egg distribution northward by 2° between 1989 and 1992, southward by 2.3° between 1998 and 1999, and northward by 1.2° from 2002 to 2003, reflected the impact of interannual ocean variability on simulated spawning habitats of sardine (Figure 4).

Spatial patterns in temperature and behavioral movement of adults were the two major factors inducing shifts in spawning habitats. First, increased temperatures during 1992, 1998 and 2003 shifted the 12–15°C isotherms (i.e., the temperature limits for spawning) northwards, favouring spawning activity in higher latitudes (Figure 4). Conversely, colder temperatures during 1989, 1999 and 2002, shifted the 12–15°C isotherms south of 32°N and restrained it north of 40°N (Figure 4). Second, in 1992, 1998 and 2003, better feeding conditions (i.e., higher I_{food}) and temperatures closer to optimal (i.e., lower I_{temp}) north of 32°N resulted in a northward shift of I_H between 34 and 40°N (Figure 5, second, third and sixth rows). Adults responded to these changing environmental conditions and followed these patterns by shifting their distribution to the north (Figure 5, fourth column) and by inference their potential spawning grounds. In cold years (1989, 1999 and 2002), favourable habitats (I_H) occurred mainly in regions south of 37°N under the combined effect of higher I_{food} and lower I_{temp} (Figure 5, first, fourth and fifth rows), resulting in a shift of adult distribution southwards between 32 and 37°N (Figure 5).

3.3 | Changes in early life-stage survival

3.3.1 | Egg and yolk-sac larval (EYS) survival

In the IBM, eggs and yolk-sac larvae had the highest natural mortality rates (M_{egg} = 0.72/day, $M_{yolk\text{-}sac\ larval}$ = 0.46/day). Their development to the first-feeding larval stage was temperature-dependent. As a result, warming temperatures shortened the EYS (egg and yolk-sac combined) stage duration (D: duration in days) and consequently increased EYS survival.[1] Annual EYS survival ranged between 0.57% and 2.05% with an average of 1.19% (Figure 6). The spatial overlap of egg super-individuals with their experienced temperature reflected the effect of spawning locations on EYS survival. During the warm year of 1992, EYS super-individuals experienced average temperature at 15.2°C and most eggs were found above 16°C

[1]Survival is defined as $S = e^{-M*D}$, where M is the mortality rate (/day) and D is the duration of the life stage (in days). Increase of M or/and D implies decrease in S.

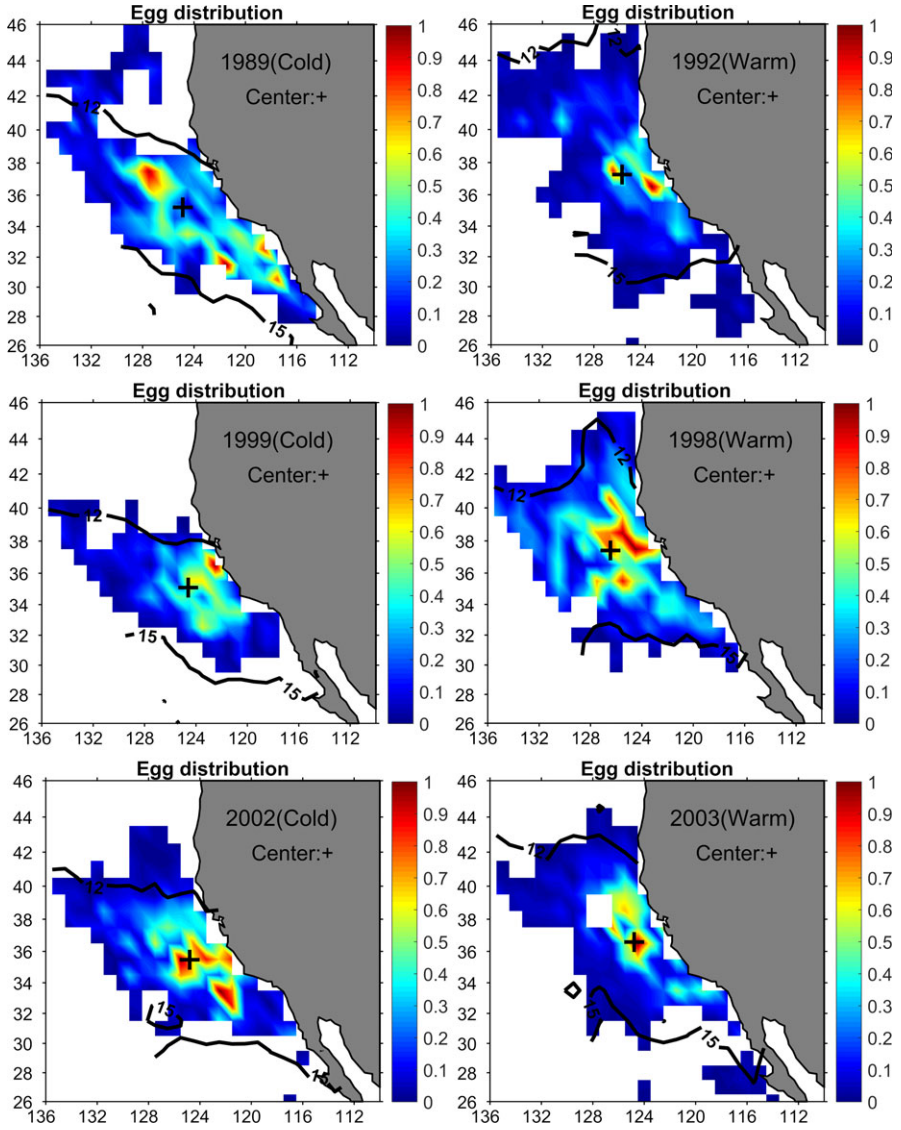

FIGURE 4 Spatial maps of egg distributions during warmer (1992, 1998, 2003) and colder (1989, 1999, 2002) years. Black lines represented 12 and 15°C isotherms, the upper and lower temperature limits for spawning. Crosses (+) denote the mean longitude and latitude of egg distribution weighted by the worth of egg super-individuals. The abundance of eggs in each grid cell was normalized to [0–1] scale using the formula: $X_{\text{norm,cell}} = \frac{X_{\text{cell}} - \min\limits_{\text{all-cells}} X}{\max\limits_{\text{all-cells}} X - \min\limits_{\text{all-cells}} X}$ [Colour figure can be viewed at wileyonlinelibrary.com]

(Figure 7). The average EYS stage duration was 6.41 days (25th percentile of 5.12 days and 75th percentile of 8 days), and survival was markedly above average (i.e., 2.05%, Figure 6). Conversely, in the cold year of 1999, egg super-individuals experienced average temperature at 13.4°C and the core of egg abundance was between 12 and 15°C (Figure 7). The average EYS stage duration was 8.41 days (25th percentile of 7.37 days and 75th percentile of 9.5 days), and survival was notably below average, (i.e., 0.50%, Figure 6). Despite colder conditions in 1989, EYS survival stayed above average (i.e., 1.55%, Figure 6); this was related to the increased presence of eggs between 36 and 38°N (Figure 4), which resulted in overlap of eggs with warm temperatures. The centre of bivariate histogram was at 14.7°C (Figure 7, dot point) and a high proportion of egg super-individuals were found between 13 and 17°C (Figure 7), preventing the drop of EYS survival in 1989. In contrast, the warmer conditions in 1998 did not assure a high EYS survival, which was below average (i.e., 0.84%. Figure 6). This occurred because spawning activity expanded in latitudes north of 38°N (Figure 4), in which temperatures were at the colder bounds of temperature range (12–15°C) for reproduction. Thus, high abundance of eggs experienced temperatures below 14°C, although average experienced temperature was around 14°C (Figure 7, dot point).

3.3.2 | Larval survival

Larval mortality rate is constant (M = 0.125/day), but the duration of larval stage (in days) is variable dependent on growth. The length threshold of 35 mm was used to determine the entrance to juvenile

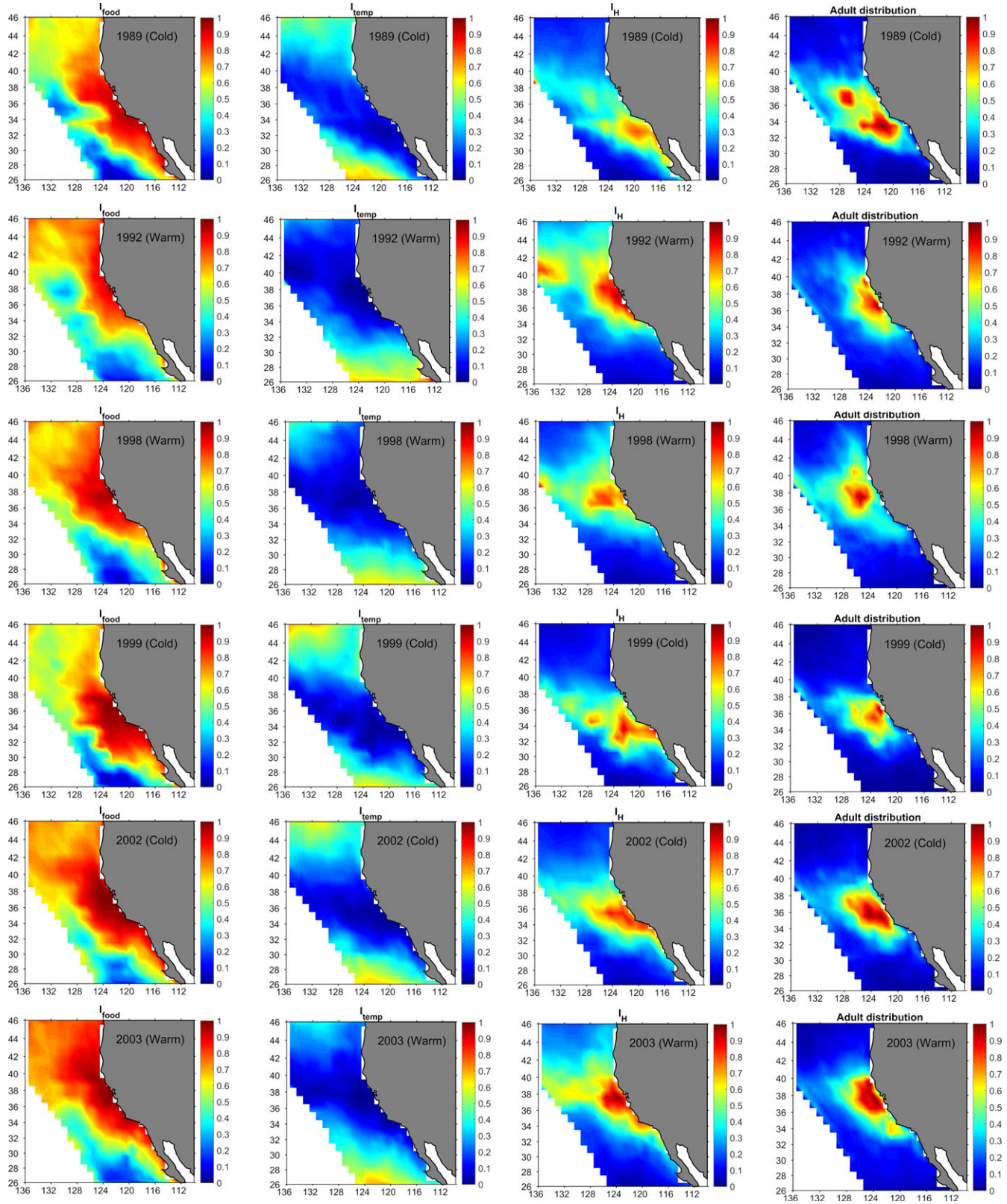

stage. Poor feeding conditions can decrease sardine larval growth rate, increase stage duration and consequently expose larvae to higher cumulative stage-specific mortality. Conversely, good larval feeding can induce fast growth and enhance survival. In the simulation, larval survival ranged from 0.116% to 0.172%, with an average of 0.149% over 1965–2006 (Figure 8). It was above average during the warmer years 1992 (0.158%) and 1998 (0.172%), and below average in 2003 (0.154%). Increased survival occurred for

FIGURE 5 Maps showing changes in the distribution of I_{food}, I_{temp}, I_H, and adult biomass during warmer (1992, 1998, 2003) and colder (1989, 1999, 2002) years. I_{food} quantified the proportion of maximum fish consumption by combining ZS, ZL, and ZP zooplankton groups through diet preferences and feeding efficiencies and ranged between 0 (poor feeding) and 1 (high feeding). I_{temp} measured the absolute deviations of temperatures experienced of adult sardines from optimal temperature T_{opt}. Low values of I_{temp} implied more favourable temperatures experienced by adult sardines. I_H was derived as the geometric mean of I_{food} and I_{temp}. I_H was high in regions where I_{food} was high and I_{temp} was low and depicted the favourable habitats for adults (I_H). All maps were normalized to [0–1] scale using the formula: $X_{norm,cell} = \frac{X_{cell} - \min_{all-cells} X}{\max_{all-cells} X - \min_{all-cells} X}$ [Colour figure can be viewed at wileyonlinelibrary.com]

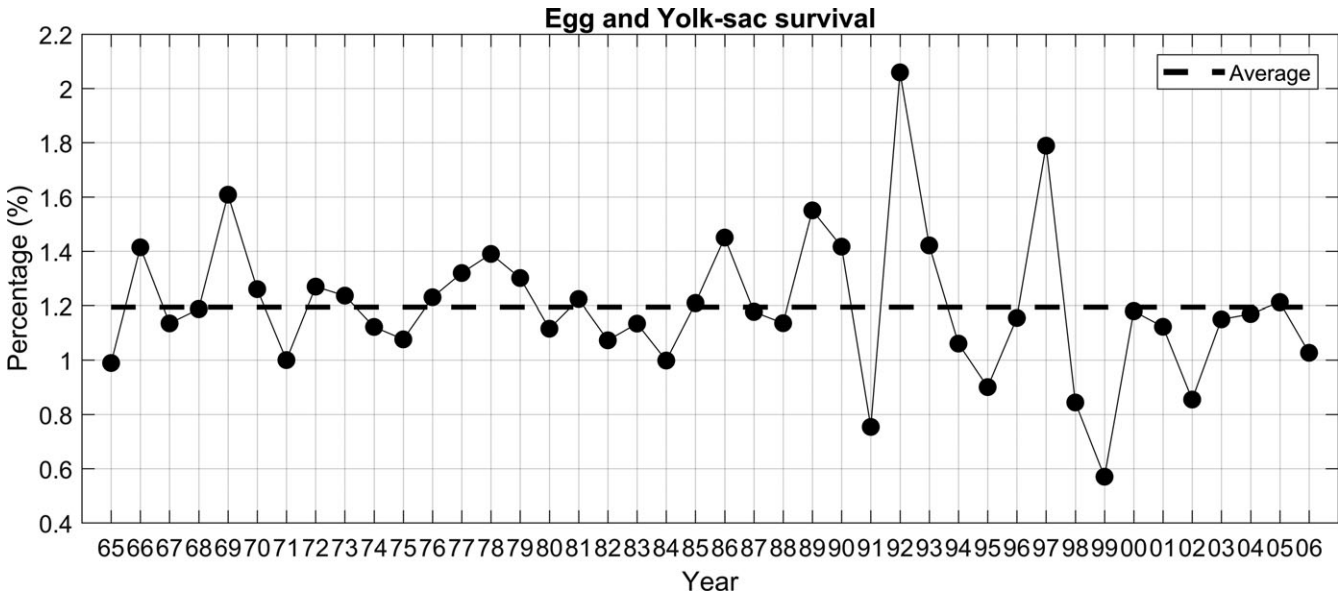

FIGURE 6 Time series of annual cumulative survival for egg and yolk-sac larval (EYS) stages over 1965–2006. Eggs and yolk-sac larvae were merged together and treated as one stage. Dashed line shows the average survival over 1965–2006

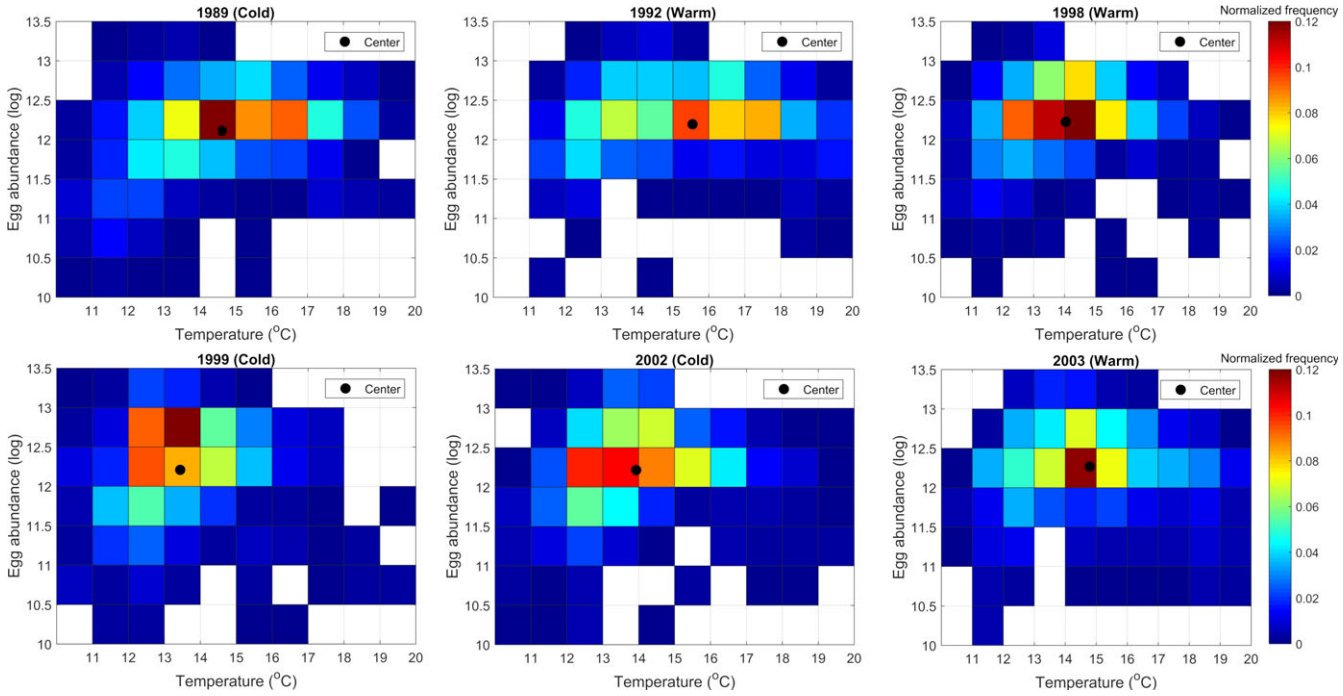

FIGURE 7 Bivariate histogram plots of egg super-individual's worth (log) against their experienced temperature for 1989, 1992, 1998, 1999, 2002 and 2003. Each tile was normalized by dividing the number of egg super-individuals in that cell with the total number of super-individuals. Dot points denote the average egg abundance (log) and experienced temperature by egg super-individuals [Colour figure can be viewed at wileyonlinelibrary.com]

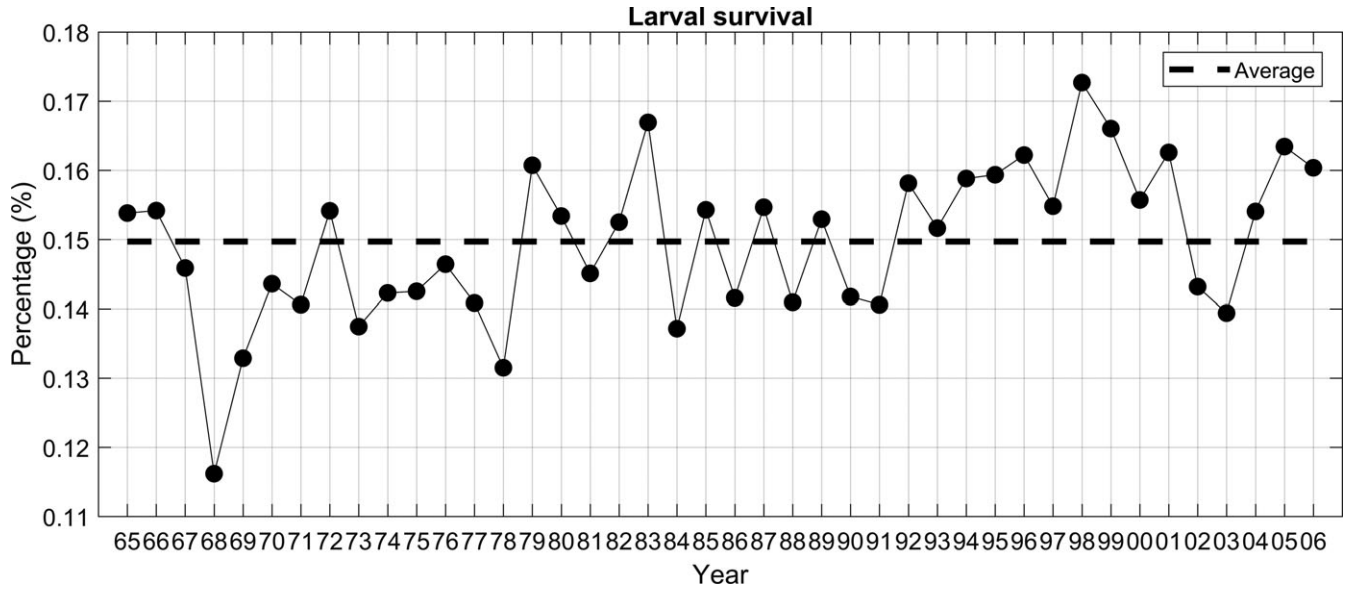

FIGURE 8 Time series of annual cumulative survival of larval sardines over 1965–2006. Dashed line shows the average survival over 1965–2006

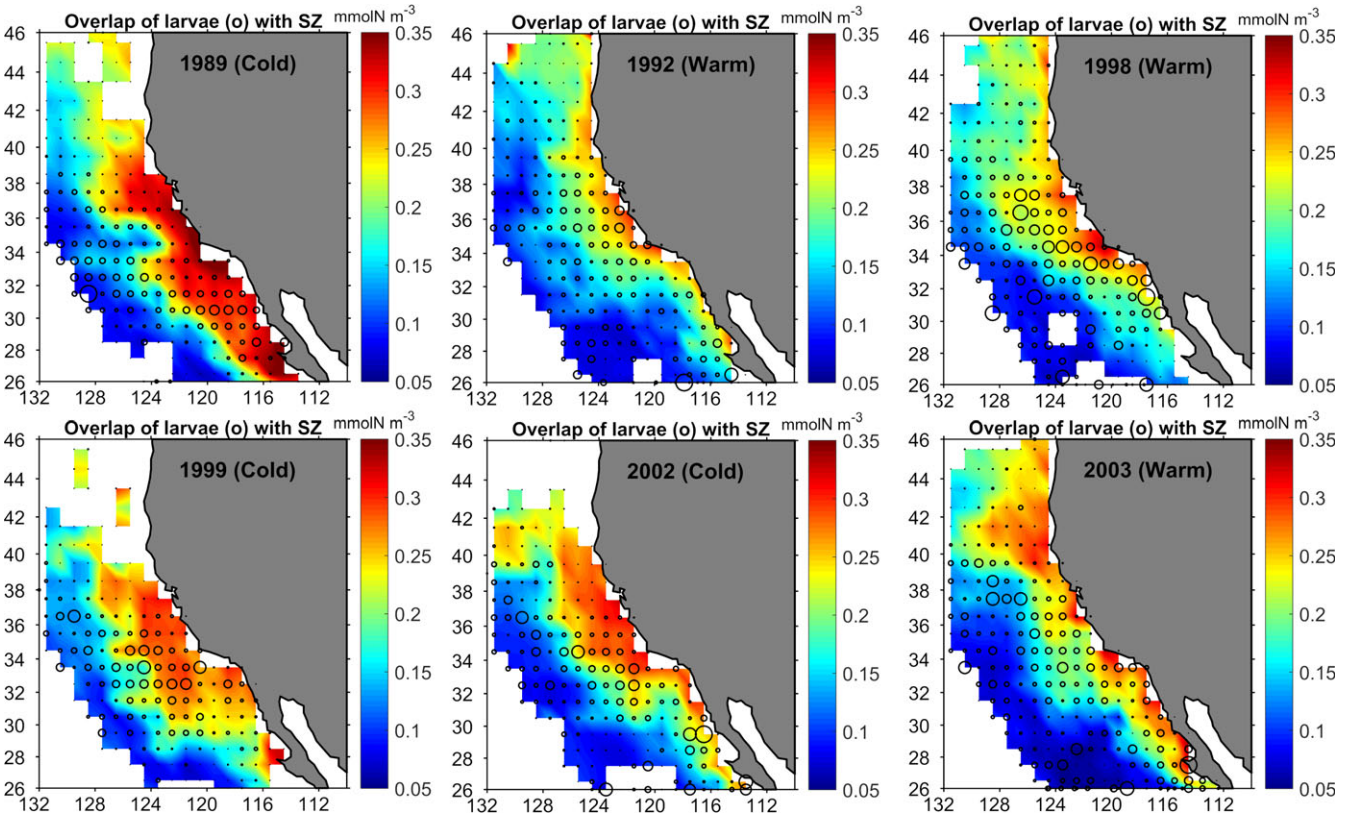

FIGURE 9 Maps of larval log-abundance (open circles) superimposed on SZ biomass for 1989, 1992, 1998, 1999, 2002 and 2003. The size of circles is proportional to log-abundance of larvae [Colour figure can be viewed at wileyonlinelibrary.com]

colder years 1989 (0.152%), and 1999 (0.166%), while survival was below average in 2002 (0.143%).

To demonstrate the potential for larvae to match with favourable feeding conditions, we averaged larval abundance maps during February–June (rearing period for larvae) using worth as a weighting factor, and then spatially overlapped them with averaged maps of experienced SZ (main prey for larvae) (Figure 9). In 1989, larvae drifted in areas south of 32°N and encountered high abundance of SZ (>0.25 mmolN/m^3), whereas those found north of 32°N and off-shore experienced poor prey conditions (<0.17 mmolN/m^3). As a

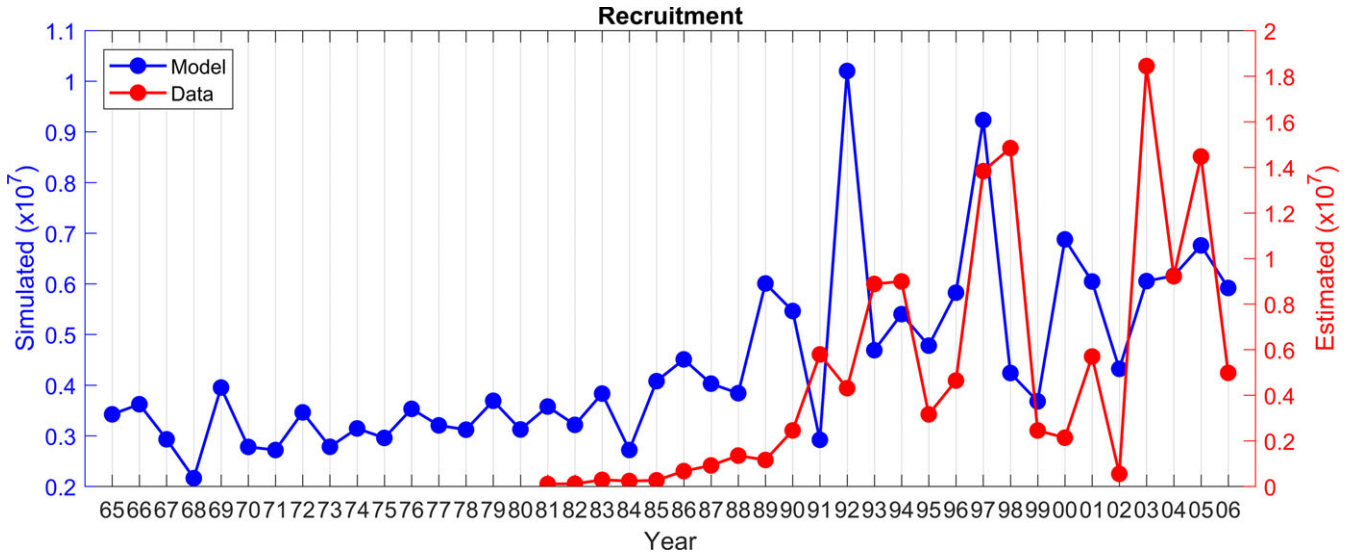

FIGURE 10 Time series of simulated (blue dots) against estimated sardine recruits (red dots) during 1965–2006. Annual simulated recruitment was the summed number of juvenile super-individuals that survived at the end of each year. Estimated recruitment shown was the average recruitment over the 2009–2016 stock assessments (Hill et al., 2017) [Colour figure can be viewed at wileyonlinelibrary.com]

result, larval survival was found slightly above average (i.e., 0.152%, Figure 8). Favourable SZ conditions (>0.2 mmolN/m^3) between 30–34°N and 118–126°W ensured good survival for larvae in 1999 despite their dispersal in offshore waters (Figure 9). In 1992 and 1998, although larvae experienced lowered SZ conditions, especially in offshore areas (western of 124°W), larval survival was found above average (Figure 8) because of the reduced offshore transport of larvae; most larvae drifted and remained inshore of 124°W assuring adequate feeding conditions (~0.2 mmolN/m^3) (Figure 9). In contrast, in 2003, the mismatch of high larval abundance with SZ, below 32°N, between 36 and 38°N and western of 124°W (<0.15 mmolN/m^3) (Figure 9), contributed to decrease in larval survival (Figure 8).

TABLE 2 Summary statistics of the regression model

Regression model	Coefficients	Std. error	t value	Pr(>|t|)	Contribution (%)
Intercept	−1.982e-06	0.028	0.000	1.0	
Egg-Prod	0.745	0.033	22.576	<2e-16	49.1
EYS-S	0.683	0.029	23.085	<2e-16	38.0
Larval-S	0.198	0.032	6.046	4.9e-07	12.9

Note. Multiple R^2: 0.96, *F*-statistic: 383.4, *p* value: <2.2e-16. Egg-Prod, egg production; EYS-S, egg and yolk-sac larval survival; Larval-S, larval survival are the explanatory variables and recruitment is the response variable.

3.4 | Temporal variation in sardine recruitment

The time series of annual simulated against estimated recruitment of sardine over 1965–2006 is shown in Figure 10. Annual recruitment ranged from 0.21 to 1.02 × 10^7 recruits per year and captured reasonably well the increase of recruitment observed in 2003 and the decrease observed in 1999 and 2002, whereas it did not agree with the observed recruitment in 1989, 1992 and 1998. In the long-term, the model showed much less interannual variation in recruitment than the estimated values; however, it aligned with the moderate variability in recruitment in early 1980s, and its intensification from the 1990s.

3.5 | Simulated sardine recruitment variability

3.5.1 | Long-term variability

The summary statistics of the regression model (1) are presented in Table 2. The standardized multiple regression coefficients demonstrated higher values for egg production (0.745) and EYS survival (0.683), which accounted for 49.1% and 38.0% of variation in recruitment. The larval survival term had the lowest coefficient (0.198) that accounted for 12.9% of the variation. The high R^2 (0.96) and metrics (*F*-statistic: 383.4, *p* value: <2.2e-16) indicated that egg production and survival during egg and larval stages can account for a large proportion of the long-term variability in recruitment. High R^2 was expected when including all explanatory factors, since annual recruitment was the result of eggs that survived during their sequential development to recruits.

The correlation coefficients between temperature and the latitudinal centre of egg distributions was $r = 0.24$ ($p = 0.01$), indicating a positive effect of increased temperature on the northward shift of spawning habitats. In contrast, there was a weak negative correlation between temperature and the longitudinal centre of egg distributions ($r = -0.2$, $p = 0.19$). There was also a positive effect of increased temperature on EYS survival; the correlation coefficient was high ($r = 0.95$, $p < 0.001$), confirming that warmer temperatures tend to shorten egg duration and therefore facilitate egg survival. For larval

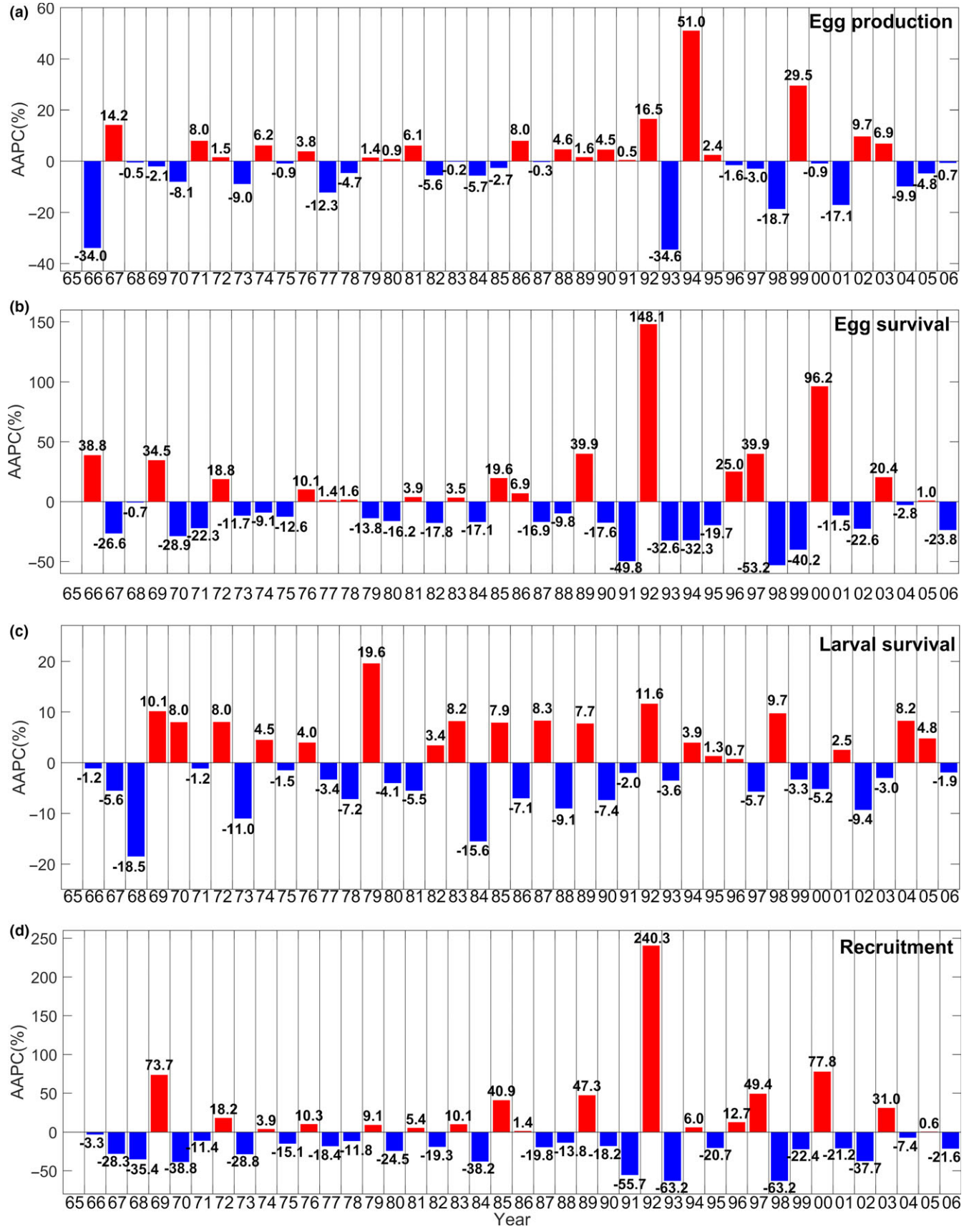

FIGURE 11 Barplots showing the anomalies in annual percent changes anomalies (AARC) of (a) egg production, (b) egg and yolk-sac larval survival, (c) larval survival, and (d) recruitment over 1960–2006 [Colour figure can be viewed at wileyonlinelibrary.com]

stage, SZ was weakly correlated with longitudinal (r = 0.06) and latitudinal (r = −0.05) centres of larval distribution. Additionally, a moderate positive relationship (r = 0.18, p = 0.23) was found between SZ and larval survival.

3.5.2 | Year-to-year variability

Year-to-year variability in egg production and early life stages survival also determined year-to-year variation in sardine recruitment, expressed as anomalies in annual percent of change (AARC) (Figure 11). In 1992, AARC displayed that recruitment increased by +240.3% and this resulted from changes in egg production of +16.5%, EYS survival of +167.6%, and larval survival of +12.0% (Figure 11). In 1998, the decrease in AARC for recruitment by −63.2% occurred because egg production decreased by −18.7%, EYS survival decreased by −58.5%, and larval survival increased by +11.1%. In 2003, the increase by +6.9% in egg production, by +28.9% in EYS survival, and the decrease by −3.1% in larval survival resulted in an increase of recruitment by +31.0%. During colder years, recruitment decreased by −22.4% in 1999 and −37.3% in 2002 due to the decrease of EYS survival by −38.1% in 1999 and −29.5% in 2002 and the decrease of larval survival by −4.3% in 1999 and −12.4% in 2002 (Figure 11).

The AARC analysis also indicated that changes in abiotic and biotic conditions were amplified across the sardine's life history and led to large changes in sardine recruitment. The coupling of the IBM with ROMS-NEMURO models showed that variation in temperature and zooplankton conditions experienced by the sardine population ranged by ±1°C (Figure 2) and ±0.2 mmolN/m^3 (Figure 3). These variations resulted in annual percent of changes from −34.6% to +51.0% for egg production (Figure 11a), from −58.5% to +167.6% for EYS survival (Figure 11b), from −20.8% to +21.7% for larval survival (Figure 11c), and from −63.2% to +240.3% for recruitment (Figure 11d). In addition, AARCs in egg production and EYS and larval survival showed that these factors act synergistically to define the amplitude of recruitment variability from 1 year to another. Thus, years with a concurrent increase of EYS and larval survival favoured recruitment (e.g., 1985, 1989, 1992, 1997) and years with a decrease in both egg and larval survival resulted in a decline in recruitment (e.g., 1999, 2002) (Figure 10d). We also had years with opposing effects of EYS and larval survival that resulted in recruitment that depended on the combined effects of these factors (e.g., 1968, 1977, 1978, 1986, 1987, 1994, 1998, 2000, 2003). In addition, years with a notable increase of egg production did not necessarily ensure an increase of recruitment (e.g., 1999, 2002) due to decreased survival of EYS or larval stages, and some years with moderate egg production had increased recruitment due to increased survival of EYS or larval stages (e.g., 1985, 1989, 1997, 2000).

EYS survival appeared as a key factor favouring or limiting recruitment success when it changed more than 20% (Figure 11). Thus, years with a significant increase in EYS survival (+29.8% in 1969, +30.8% in 1989, +167.6% in 1992, +22.7% in 1996, +49.2% in 1997, +101.3% in 2000, +28.4% in 2003) (Figure 11b) resulted in better recruitment (Figure 11d). Conversely, years with a large decrease in egg survival (−52.5% in 1991, −36.6% in 1993, −58.5% in 1998, −38.1% in 1999, −29.5% in 2002, −21.0% in 2006) (Figure 11b) resulted in a notable decrease in decrease of recruitment (Figure 11d). One notable exception was in 1994, in which the decrease of EYS survival by −31.0% (Figure 11b) was compensated by a high increase in egg production by +51%, resulting in a slight increase in recruitment of +6.0%.

4 | DISCUSSION

Model analysis confirmed that changes in environmental conditions, predicted by ROMS-NEMURO submodels, in combination with the life history and habitat characteristics of sardine represented by the IBM (offshore distribution, feeding preference on smaller prey types, behavioral movement), had a considerable effect on sardine recruitment.

Figure 12 illustrated how temperature and zooplankton conditions experienced by juvenile and adult sardines were related to whole domain averages. Sardines individuals occupy a subset of the domain and have a behavior aiming to reach their optimal habitats. The model domain exhibited temperatures who were higher on average by 3.08°C compared to sardine habitats, due to its wide coverage including regions with temperatures above 20°C (not shown), while behavioral movement helped sardine individuals to access and remain near their optimal thermal conditions, i.e., between 13 and 14°C (Figure 12a). The strong correlation between model domain and experienced temperature anomalies (r = 0.77) showed that sardines followed closely the interannual variation in temperature (Figure 12b).

Sardines responded to changes in zooplankton biomass through their consumption rate, expressed through p value (ranging from 0 meaning poor feeding to 1 meaning high feeding). Sardines encountered better feeding conditions (e.g., higher p value) within their habitats compared to the model domain average (Figure 12c), which includes areas with very low zooplankton biomass (not shown). The high correlation (r = 0.7) between model domain and experienced p-value illustrated that sardines aligned with interannual changes in zooplankton conditions, but they succeeded to ensure the maximum possible consumption using their behavioral movement towards their favourable habitats.

Our analysis pointed out the importance of spatial processes in regulating the early life history of sardine. Following distributional changes in temperature and prey conditions, adult sardines defined the spatial differences in spawning habitats and future environmental conditions for offsprings. Temperature experienced by EYS super-individuals was within the ranges of their physiological tolerance. It was, however, the spatial match of eggs with temperature that affected substantially the survival of these stages. Then, larval drift due to circulation patterns and the match-mismatch of larvae with their prey affected larval growth and consequently their survival.

Changes in the geographic ranges of spawning were driven by spatial variations in temperature and the behavioral movement of

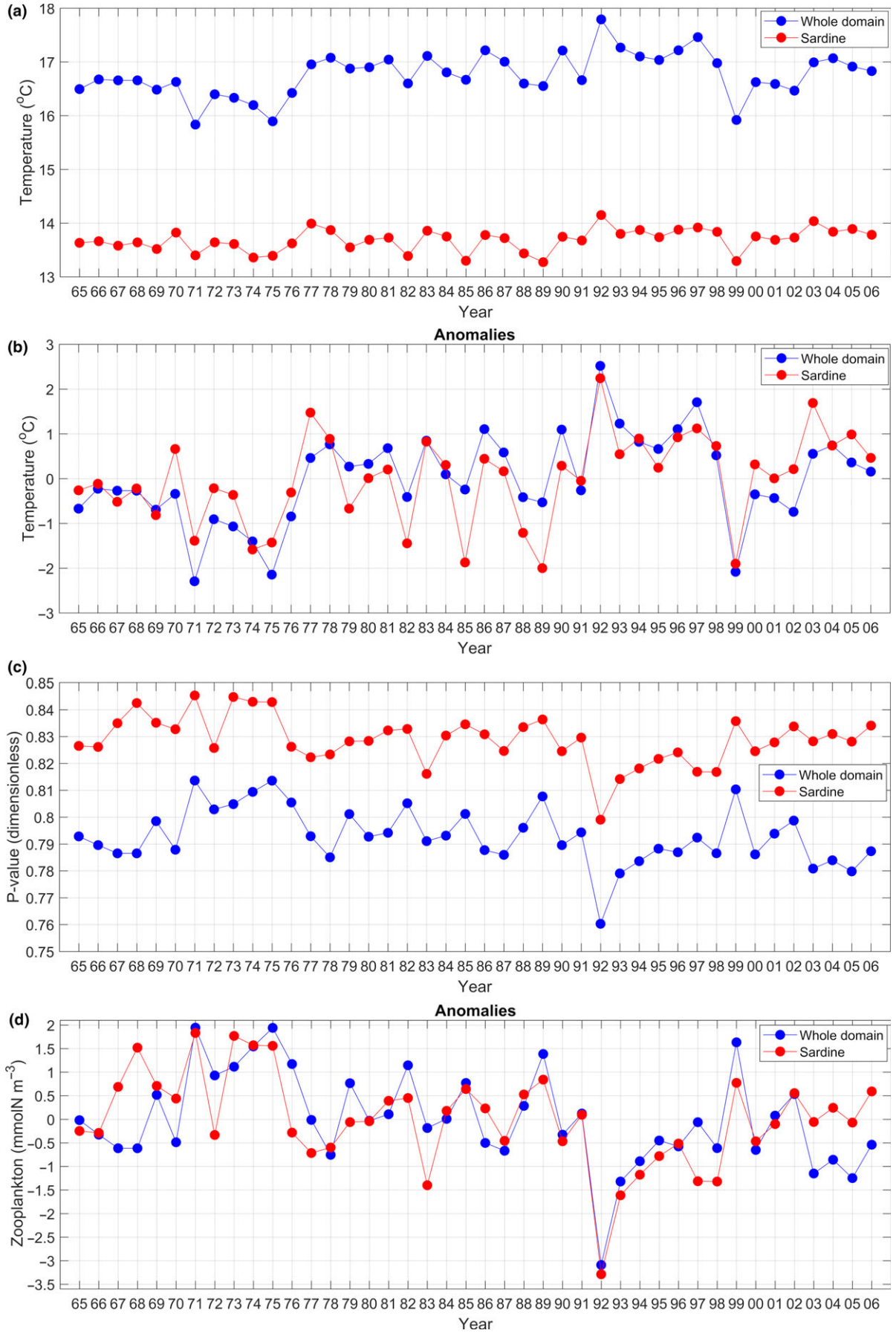
(a)
Temperature (°C)
Whole domain
Sardine
Year
(b)
Anomalies
Temperature (°C)
Whole domain
Sardine
Year
(c)
P-value (dimensionless)
Whole domain
Sardine
Year
(d)
Anomalies
Zooplankton (mmolN m⁻³)
Whole domain
Sardine
Year

FIGURE 12 Annual average temperature calculated over 0–30 m and the whole domain against averaged temperature experienced from juvenile and adult sardines, presented as (a) actual values and (b) anomalies. Similarly, annual average consumption rate (expressed through *p* value) calculated over 0–30 m and the whole domain against experienced *p* value from juvenile and adult sardines, presented as (c) actual values and (d) anomalies. Anomalies were computed as: (value-mean)/standard-deviation over 1965–2006 [Colour figure can be viewed at wileyonlinelibrary.com]

adult sardines. Warming conditions favoured the shift of spawning north of 37°N and decreased spawning activity south of 34°N, as adults moved to find optimal habitat in terms of food and temperature. These northward shifts agreed with Agostini et al. (2007) and McClatchie (2014) who hypothesized that the centre of sardine spawning shifts north in warmer than average years due to access the most favourable habitat in regard to temperature and food, compare to colder periods.

Regression analysis suggested that egg production was the most influential factor to control the long-term variability in sardine recruitment during 1965–2006 of the historical simulation. On the other hand, egg production did not dominate on defining the year-to-year variation in recruitment. AARC analysis illustrated that the number of eggs produced and the survival of egg and larval stages acted synergistically to determine the magnitude of interannual change in recruitment rate. This agrees conceptually with Pepin and Marshall (2015) and Houde (2008), who highlighted that the combined action of several factors on different time and space scales throughout the pre-recruit life can determine recruitment success. Concurrently, interannual amplifications of larval survival were moderate (Figure 11c), despite the offshore dispersal of larvae. This can be attributed to the main preference of larval feeding on SZ in the model, which prevented very low consumption, despite the offshore larval distribution. This broadly agreed with existing knowledge that sardines appear to feed on smaller prey items and be advected in offshore areas (Rykaczewski & Checkley, 2008; Weber et al., 2015).

Observed distribution and abundance of sardine eggs from the CalCOFI surveys are plotted for years 1998, 1999, 2002 and 2003 (Figure 13). In 1998 and 2003, eggs were found closer to shore, occupied a smaller spawning area, the proportion of total egg abundance south of 34°N was 38.0% in 1998 and 41.1% in 2003, and part of spawning activity was located north of 36°N (Figure 13). Conversely, in cold years 1999 and 2002, more eggs were found offshore and south of 34°N (57.5% in 1999 and 59.1% in 2002), and little spawning occurred north of 36°N. Simulated egg distributions captured qualitatively the north-to-south shift of spawning activity observed in data between warm and cold years. The percent of eggs found south of 34°N was 15.6% in 1998 and 23.8% in 2003 and increased to 42.1% in 1999 and 33.4% in 2002 (Figure 4).

Larval distribution of sardines in the IBM was largely determined by spawning location and advection during egg and larval stages. IBM results showed that larvae in 1998 were distributed more inshore (30–36°N) and north of 34°N compare to 1999 (Figure 9). This is in general agreement with observed distribution of larvae in 1998, which was more north of 34°N and alongside the shore compare to 1999 (Figure 14). However, contrary to observed larvae data, modelled larvae were found more offshore between 36 and 38°N in 1998 and western of 124°W in 1999. Furthermore, both in the model and data, larvae were located more to the north of 34°N in warmer 2003 compare to colder 2002 (Figures 8 and 14).

Model analysis showed that sardines recruited well during the warm years 1992 and 2003 (identified also as El Niño events), despite having experienced less favourable prey conditions compared to other years (Figure 3). This conclusion was corroborated with other studies reporting that Californian sardine appears to benefit during El Niño episodes and ensure good recruitment, although

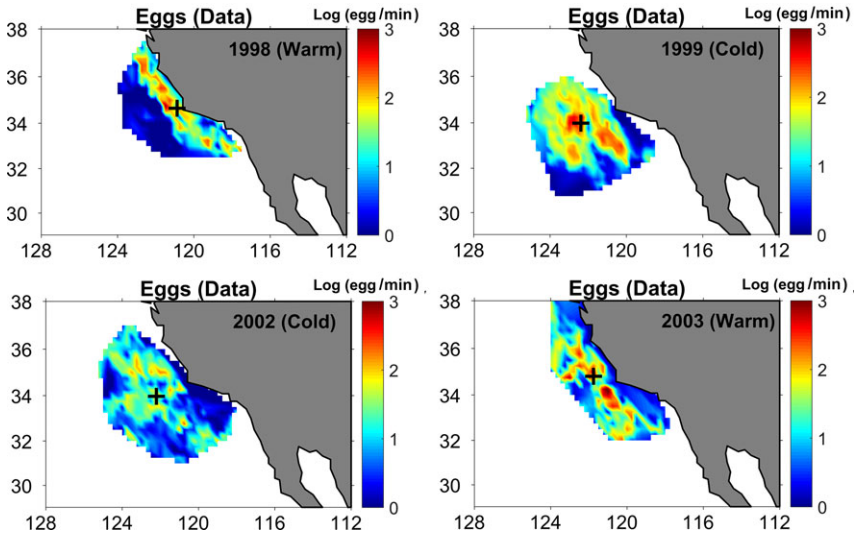

FIGURE 13 Distribution and abundance of sardine eggs collected during CalCOFI surveys (http://calcofi.org/data.html) for 1998, 1999, 2002 and 2003. Black crosses show the centre of gravity (i.e., longitude, latitude) of the distributions [Colour figure can be viewed at wileyonlinelibrary.com]

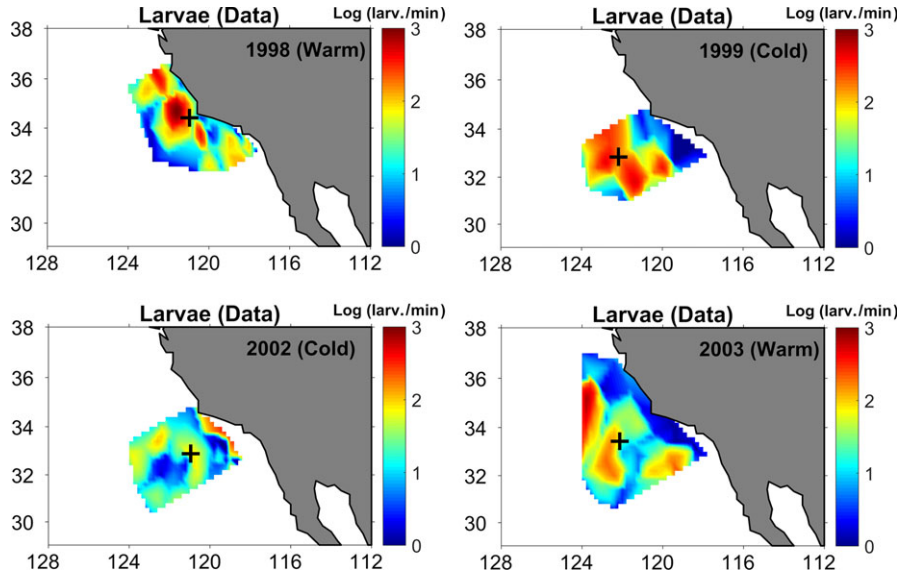

FIGURE 14 Distribution and abundance of sardine larvae collected in CalCOFI programme (http://calcofi.org/) for 1998, 1999, 2002 and 2003. Black crosses show the centre of gravity (i.e., longitude, latitude) of the distributions [Colour figure can be viewed at wileyonlinelibrary.com]

they are characterized by lowered ocean productivity (Bakun & Broad, 2003; Jacobson & MacCall, 1995; Lluch-Belda, Lluch-Cota, Hernandez-Vazquez, & Salina-Zavala, 1991). However, these studies did not provide a mechanism for good recruitment.

Our mechanistic analysis is consistent with a hypothesis that could explain strong recruitment for sardine. Decreased prey conditions occurred during warmer years were compensated by the shift of spawning to optimal habitats (close to optimal temperature and richest feeding grounds) through adult behavioral movement, a positive effect of rising temperature on EYS survival, and the spatial match of larvae with adequate SZ biomass more closely along the coast, which prevented a drop of larval survival. Our explanation agreed with the existing hypothesis that sardine reproductive success may be improved when reproductive habitat shifts northward due to increased food concentration for larvae (Agostini et al., 2007). Additionally, our findings revealed that the synergistic act of several processes was responsible for this successful recruitment. The hypothesis that reproductive success during warm years may also be the result of decreased predation pressure on early life-history stages (Agostini et al., 2007; Bakun & Broad, 2003) could not be tested by the model, since egg and larval mortality rates did not consider explicitly the effect of predation.

The juvenile stage of a fish species has been acknowledged as determinant to alter the strength of a year class due to its long duration, which can last for many months (Bradford & Cabana, 1997; Pepin & Marshall, 2015). Juvenile mortality rate was constant in the IBM (i.e., 0.011/day). The transition to subadult stage occurred at the end of the year. Therefore, the juvenile stage could not be prolonged under poor feeding conditions. Its duration depended on the timing of egg release and the duration of larval stage. Thus, the earlier the egg production occurred and the shorter the duration of the larval stage, the lower the juvenile survival, since juveniles hatched earlier, and their stage lasted longer. Due to dependency of juvenile survival on larval survival, we did not include it as an explanatory variable in the regression model and AARC analysis. To account for the effect of environment on annual juvenile survival, we adjusted juvenile survival using the juvenile growth rate as a proxy. Thus, after considering the average length of recruits (mm) over 1965–2006 as the reference length, we subtracted the annual mean length of recruits from the reference length and we divided it by the average juvenile growth rate (mm/day) of that year. This determined the greater or fewer days needed for juveniles to reach the reference length in a particular year. These days were used to recalculate juvenile survival, which increased (decreased) when less (more) days needed. Calculating the correlation between adjusted juvenile survival and recruitment, we got a low value of $r = 0.07$ ($p = 0.62$). Conversely, there was a significant correlation between adjusted juvenile survival and the biomass of adult sardines ($r = 0.46$, $p = 0.001$), implying that juveniles may have an indirect effect on recruitment through their control on spawning stock biomass of the population.

Due to the high complexity of the end-to-end model used here, several sources of uncertainties impose limitations to its explanatory capability. First, contrary to observed egg distributions (Figure 13), simulated distribution of eggs extended west of 124°W in 1998, 1999, 2002 and 2003 (Figure 4). This discrepancy can be attributed to the assumptions of the reproduction in the model. Egg release was based on temperature and the somatic and feeding conditions of the parents. Nevertheless, in the CCS, sardines may avoid releasing eggs in regions with strong wind-driven Ekman transport that could induce offshore transport (McClatchie, 2014) and seem to have an affinity to intermediate values of upwelling (Lluch-Belda

et al., 1991). The IBM did not take into consideration physical processes that may affect spawning behavior of sardine. Understanding the effects of these processes on spawning activity needs further consideration.

Simulated recruitment captured, to some degree, the interannual variation in recruitment estimated from data. For instance, the increase of recruitment in 2003 and its decrease in 1999 and 2002 were in good agreement with the estimated recruitment (Figure 10). In contrast, simulated recruitment did not match estimated recruitment for 1989, 1992, and 1998. A major source of uncertainty, affecting simulated recruitment, was related to assumed mortality rates of early life stages. Natural mortality rates were set constant in the IBM, whereas field measurements have shown that these rates are highly variable spatially and interannually (Butler, 1991; Isaacs, 1965; Lo, Macewicz, & Griffith, 2005; Lo, Smith, & Butler, 1995). With regard to juveniles, their predefined transition to subadults at the end of each year did not allow the extension of their stage into the next year due to climate variability. Under this simplified assumption, juvenile growth could not strongly affect juvenile survival, and by inference, regulate recruitment strength. Future refinement of the model should consider variability in juvenile survival under a changing environment because juvenile stage may significantly influence recruitment success or failure of marine fishes due to its long duration (often $>$ 1 year) (Houde, 2008). Adding elevated juvenile mortality due of slow growing individuals (Okunishi et al., 2012) could be an option.

Another major source of uncertainty was the movement algorithm applied in the model. Simulating fish movement in a spatially-explicit environment in 3D is a challenging issue because the underlying mechanisms driving fish behavioral movement are uncertain, and calibration data to evaluate its predictive capability are limited. This has resulted in the development of different approaches for representing how fish individuals perceive and respond to their environment (Watkins & Rose, 2013). The kinesis approach (Humston et al., 2004; Okunishi, Yamanaka, & Ito, 2009; Politikos, Huret, & Petitgas, 2015) used here was based on temperature and food as cues to define how close an individual was to its optimal conditions. Additionally, model-forced northward migration to feeding grounds was imposed during July–September. Ideally, feeding migration would be an emergent property so that it can respond to environmental variation. However, our current lack of knowledge (e.g., what are the cues) and the resolution of the model (coarse for some gradients) resulted in us forcing migration in this version of the model.

The recruitment analysis presented here investigated bottom-up controls (i.e., the effects of variation of physical and planktonic conditions) on sardine recruitment. We did not investigate variation in recruitment due to top-down processes (predation and fishing) and thus the significance of top-down effects on recruitment remains an open question. Simulated predation in the model had only small year-to-year differences on population dynamics and fishing resulting from fleet sub model resulted in removals mostly controlled by adult abundance (Fiechter, Rose et al., 2015; Rose et al., 2015). All of this suggests a need for improvement before the model can be used to explore the top-down impact of predation and fishing dynamics on sardine recruitment. Moreover, potential density-dependent factors related to competition for prey (Houde, 2008) and constraint of egg production when egg abundance is high (Ganias, 2014), were not explicitly parameterized in the end-to-end model. Such processes have been identified as important for improving the match of modelled and observed spawning-stock relationships for sardine and for generating more realistic long-term simulations (Rose et al., 2015).

Our main goal was to mechanistically explore the effect of climate on sardine habitats, survival and recruitment using an end-to-end model, with a focus on ENSO events. ENSO is the largest mode of climate variability characterized by the model. Thus, the examination of extreme years (i.e., El Niño and La Niña) was a good means to infer how sardines responded to temporally and spatially varying physical (e.g., temperature) and biological (e.g., prey) conditions. Similar analysis approach has been adopted by several IBMs, whereby they attempt to link environmental factors to fish growth (Fiechter, Huff et al., 2015; Siddon et al., 2013), survival (Daewel, Peck, & Schrum, 2011; Petrik, Ji, & Davis, 2014), and recruitment (Siddon et al., 2013; Xu et al., 2013) between years with markedly different oceanic conditions.

Fiechter, Rose et al. (2015) used the model outputs of Rose et al. (2015) to perform a correlation analysis. They related annual abundances of adult sardine to lagged annual age-0 (egg through juvenile) survival rates to total annual egg production. They also used regression analysis to identify linkages between major leading modes of variability in the Northeast Pacific (i.e., Pacific Decadal Oscillation [PDO]; North Pacific Gyre Oscillation [NPGO]; NINO 3.4 index [ENSO] and the Bakun Upwelling Index) to sardine survival and growth. Here, we conducted further correlations to identify the long-term relationships between environmental conditions and the time series of EYS and larval survival and the gravity centres of their distribution. These correlations generally agreed with the mechanistic analysis performed for El Niño years; warming conditions tended to shift northward egg distributions and favour egg and larval survival.

Despite years of research in linking environmental drivers to early life growth, mortality and recruitment of fish populations (Pepin & Marshall, 2015), a mechanistic understanding of the recruitment variability remains elusive and continues to be a worthy goal (Bakun & Broad, 2003; Checkley et al., 2017). Our analysis approach provided an example of how an end-to-end fish model can move beyond correlations and provide a cause-and-effect understanding on the relationship amongst climate variability, fish habitats and population variability by linking multiple recruitment hypotheses (Hare, 2014).

To conclude, concern persists about the status of sardine stock in the CCS, since it has declined by more than 90% since 2007, reaching its lowest biomass levels in decades (Hill et al., 2017). It is believed that this dramatic decline is related to changing environment and exacerbated by overfishing (Essington et al., 2015; Lindegren & Checkley, 2013). Thus, continuing the effort to improve our understanding what drives sardine productivity remains a critical issue in our study region for better managing the stock and preventing its collapse.

ACKNOWLEDGEMENTS

We thank Dr Sam McClatchie for providing us access to egg distribution data from CUFES samples of CalCOFI surveys, and Dr Kevin Hill and Dr Juan Zwolinski for our valuable discussion during the comparison of the model with recruitment data.

CONFLICT OF INTEREST

The authors declare no conflict of interest.

ORCID

Dimitrios V. Politikos http://orcid.org/0000-0002-9955-2184

REFERENCES

Agostini, V. N., Bakun, A., & Francis, R. C. (2007). Larval stage controls on Pacific sardine recruitment variability: High zooplankton abundance linked to poor reproductive success. *Marine Ecology Progress Series*, *345*, 237–244. https://doi.org/10.3354/meps06992

Alheit, J., Roy, C., & Kifani, S. (2009). Chapter 3: Decadal-scale variability in populations. In D. M. Checkley, J. Alheit, & Y. Oozeki (Eds.), *Climate change and small pelagic fish* (pp. 285–383). Cambridge, UK: Cambridge University Press. https://doi.org/10.1017/CBO9780511596681

Asch, R., & Checkley, D. M. Jr (2013). Dynamic height: A key variable for identifying the spawning habitat of small pelagic fishes. *Deep-Sea Research. Part I, Oceanographic Research Papers*, *171*, 79–91. https://doi.org/10.1016/j.dsr.2012.08.006

Bakun, A., & Broad, K. (2003). Environmental 'loopholes' and fish population dynamics: Comparative pattern recognition with focus on El Niño effects in the Pacific. *Fisheries Oceanography*, *12*, 458–473. https://doi.org/10.1046/j.1365-2419.2003.00258.x

Bradford, M. J., & Cabana, G. (1997). Chapter 17: interannual variability in stage-specific survival rates and the causes of recruitment variation. In R. C. Chambers, & E. A. Trippel (Eds.), *Early life history and recruitment in fish populations* (pp. 469–493). London: Chapman and Hall. https://doi.org/10.1007/978-94-009-1439-1

Butler, J. L. (1991). Mortality and recruitment of Pacific sardine, *Sardinops sagax caerulea*, larvae in the California Current. *Canadian Journal of Fisheries and Aquatic Science*, *48*, 1713–1723. https://doi.org/10.1139/f91-203

Chavez, F. P., Ryan, J., Lluch-Cota, S. E., & Niquen, M. (2003). From anchovies to sardines and back: Multidecadal change in the Pacific Ocean. *Science*, *299*, 217–221. https://doi.org/10.1126/science.1075880

Checkley, D. M. Jr, Asch, R. G., & Rykaczewski, R. R. (2017). Climate, Anchovy, and Sardine. *Annual Review of Marine Science*, *9*, 469–493. https://doi.org/10.1146/annurev-marine-122414-033819

Chevan, A., & Sutherland, M. (1991). Hierarchical partitioning. *American Statistician*, *45*, 90–96.

Cushing, D. H. (1974). The natural regulation of fish populations. In F. R. Harden Jones (Ed.), *Sea fisheries research* (pp. 399–412). London: Elek Science.

Daewel, U., Peck, M. A., & Schrum, C. (2011). Life history strategy and impacts of environmental variability on early life stages of two marine fishes in the North Sea: An individual-based modelling approach. *Canadian Journal of Fisheries and Aquatic Sciences*, *68*, 426–443. https://doi.org/10.1139/F10-164

Essington, T. E., Moriarty, P. E., Froehlich, H. E., Hodgson, E. E., Koehn, L. E., Oken, K. I., … Stawitz, C. C. (2015). Fishing amplifies forage fish population collapses. *Proceedings of the National Academy of Sciences*, *112*, 6648–6652. https://doi.org/10.1073/pnas.1422020112

Fiechter, J., Huff, D. D., Martin, B. T., Jackson, D. W., Edwards, C. A., Rose, K. A., … Wells, B. K. (2015). Environmental conditions impacting juvenile Chinook salmon growth off central California: an ecosystem model analysis. *Geophysical Research Letters*, *42*, 2910–2917. https://doi.org/10.1002/2015GL063046

Fiechter, J., Rose, K. A., Curchitser, E. N., & Hedstrom, K. S. (2015). The role of environmental controls in determining sardine and anchovy population cycles in the California Current: Analysis of an end-to-end model. *Progress in Oceanography*, *138*, 381–398. https://doi.org/10.1016/j.pocean.2014.11.013

Galindo-Cortes, G., De Anda-Montanez, J. A., Arreguin-Sanchez, F., Salas, S., & Balart, E. F. (2010). How do environmental factors affect the stock-recruitment relationship? The case of the Pacific sardine (*Sardinops sagax*) of the northeastern Pacific Ocean. *Fisheries Research*, *102*, 173–183. https://doi.org/10.1016/j.fishres.2009.11.010

Ganias, K. (2014). *Biology and ecology of anchovies and sardine*. Boca Raton, FL: CRC Press, Taylor Francis Group.

Garćia-Garćia, L. M., Ruiz-Villarreal, M., & Bernal, M. (2016). A biophysical model for simulating early life stages of sardine in the Iberian Atlantic stock. *Fisheries Research*, *173*, 250–272.

Groemping, U. R. (2010). *Package 'relaimpo'*. Retrieved from: https://cran.r-project.org/web/packages/relaimpo/relaimpo.pdf.

Haidvogel, D. B., Arango, H., Budgell, W. P., Cornuelle, B. D., Curchitser, E., Di Lorenzo, E., … Wilkin, J. (2008). Ocean forecasting in terrain-following coordinates: Formulation and skill assessment of the Regional Ocean Modeling System. *Journal of Computational Physics*, *227*, 3595–3624. https://doi.org/10.1016/j.jcp.2007.06.016

Hare, J. A. (2014). The future of fisheries oceanography lies in the pursuit of multiple hypotheses. *ICES Journal of Marine Science*, *71*, 2343–2356. https://doi.org/10.1093/icesjms/fsu018

Hargreaves, N. B., Ware, D. M., & McFarlane, G. A. (1994). Return of Pacific sardine (*Sardinops sagax*) to the British Columbia coast in 1992. *Canadian Journal of Fisheries and Aquatic Science*, *51*, 460–463. https://doi.org/10.1139/f94-048

Hill, K. T., Crone, P. R., & Zwolinski, J. P. (2017). *Assessment of the Pacific sardine resource in 2017 for U.S. management in 2017-18*. Pacific Fishery Management Council, April 2017 Briefing Book, Agenda Item G.5.a, Portland, Oregon. 146 pp.

Hjort, J. (1926). Fluctuations in the year classes of important food fishes. *Journal du Conseil International pour l'Exploration de la Mer*, *1*, 5–38. https://doi.org/10.1093/icesjms/1.1.5

Hocke, K., & Kämpfer, N. (2011). Hovmöller diagrams of climate anomalies in NCEP/NCAR reanalysis from 1948 to 2009. *Climate Dynamics*, *36*, 355–364. https://doi.org/10.1007/s00382-009-0706-5

Houde, E. D. (2008). Emerging from Hjort's Shadow. *Journal of Northwest Atlantic Fishery Science*, *41*, 53–70. https://doi.org/10.2960/J.v41.m634

Humston, R., Olson, D. B., & Ault, J. S. (2004). Behavioral assumptions in models of fish movement and their influence on population dynamics. *Transactions of the American Fisheries Society*, *133*, 1304–1328. https://doi.org/10.1577/T03-040.1

Isaacs, J. D. (1965). Larval sardine and anchovy interrelationships. *California Cooperative Oceanic Fisheries*, *10*, 102–140.

Jacobson, L., & MacCall, A. D. (1995). Stock-recruitment models for Pacific sardine (*Sardinops sagax*). *Canadian Journal of Fisheries and Aquatic Science*, *52*, 566–577. https://doi.org/10.1139/f95-057

King, J. R. (Ed.) (2005). *Report of the study group on the fisheries and ecosystem responses to recent regime shifts*. PICES Scientific Report Number 28. North Pacific Marine Science Organization (PICES),

Institute of Ocean Sciences, Sidney, BC, P. 168. Retrieved fom https://www.pices.int/publications/scientific_reports/Report28/Rep_28_FERRRS.pdf

Kishi, M. J., Kashiwai, M., Ware, D. M., Megrey, B. A., Eslinger, D. L., Werner, F. E., … Zvalinsky, V. I. (2007). NEMURO - a lower trophic level model for the North Pacific marine ecosystem. *Ecological Modelling*, *202*, 12–25. https://doi.org/10.1016/j.ecolmodel.2006.08.021

Kristiansen, T., Drinkwater, K. F., Lough, R. G., & Sundby, S. (2011). Recruitment variability in North Atlantic Cod and Match-Mismatch dynamics. *PLoS ONE*, *6*, e17456. https://doi.org/10.1371/journal.pone.0017456

Lindegren, M., & Checkley, D. M. Jr (2013). Temperature dependence of Pacific sardine (*Sardinops sagax*) recruitment in the California Current Ecosystem revisited and revised. *Canadian Journal of Fisheries and Aquatic Sciences*, *70*, 245–252. https://doi.org/10.1139/cjfas-2012-0211

Lindegren, M., Checkley, D. M. Jr, Rouyer, T., MacCall, A. D., & Stenseth, N. C. (2013). Climate, fishing and fluctuations of sardine and anchovy in the California Current. *PNAS*, *110*, 13672–13677. https://doi.org/10.1073/pnas.1305733110

Lluch-Belda, D., Crawford, R. J. M., Kawasaki, T., MacCall, A. D., Parrish, R. H., Schwartzlose, R. A., & Smith, P. E. (1989). World-wide fluctuations of sardine and anchovy stocks: The regime problem. *African Journal of Marine Science*, *8*, 195–205. https://doi.org/10.2989/02577618909504561

Lluch-Belda, D., Lluch-Cota, D., Hernandez-Vazquez, S., & Salina-Zavala, C. (1991). Sardine and anchovy spawning as related to temperature and upwelling in the California Current system. *California Cooperative Oceanic Fisheries Investigations Report*, *32*, 105–111.

Lo, N. C. H., Macewicz, B. J., & Griffith, D. A. (2005). Spawning biomass of Pacific sardine (*Sardinops sagax*) from 1994–2004. *CalCOFI Reports*, *46*, 93–112.

Lo, N. C., Smith, P. E., & Butler, J. L. (1995). Population growth of northern anchovy and Pacific sardine using stage-specific matrix models. *Marine Ecology Progress Series*, *127*, 15–26. https://doi.org/10.3354/meps127015

Logerwell, E., Lavaniegos, B., & Smith, P. (2001). Spatially-explicit bioenergetics of Pacific sardine in the Southern California Bight: Are mesoscale eddies areas of exceptional production? *Progress in Oceanography*, *49*, 391–406. https://doi.org/10.1016/S0079-6611(01)00032-5

MacCall, A. D. (2009). Mechanisms of low-frequency fluctuations in sardine and anchovy populations. In D. M. Checkley Jr, J. Alheit, Y. Oozeki, & C. Roy (Eds.), *Climate change and small pelagic fish* (pp. 285–299). New York, NY: Cambridge University Press. https://doi.org/10.1017/CBO9780511596681

McClatchie, S. (2014). *Regional fisheries oceanography of the California Current system* (p. 235). Dordrecht, the Netherlands: Springer. https://doi.org/10.1007/978-94-007-7223-6

Murphree, T., & Reynolds, C. (1995). El Niño and La Niña effects on the northeast Pacific: The 1991-1993 and 1988-1989 events. *California Cooperative Oceanic Fisheries Investigations Report*, *36*, 45–56.

Okunishi, T., Ito, S., Hashioka, T., Sakamoto, T. T., Yoshie, N., Sumata, H., … Yamanaka, Y. (2012). Impacts of climate change on growth, migration and recruitment success of Japanese sardine (*Sardinops melanostictus*) in the western North Pacific. *Climate Change*, *4*, 485–503. https://doi.org/10.1007/s10584-012-0484-7

Okunishi, T., Yamanaka, Y., & Ito, S.-I. (2009). A simulation model for Japanese sardine (*Sardinops melanostictus*) migrations in the western North Pacific. *Ecological Modelling*, *220*, 462–479. https://doi.org/10.1016/j.ecolmodel.2008.10.020

Ospina-Alvarez, A., Catalan, I. A., Bernal, M., Roos, D., & Palomera, I. (2015). From egg production to recruits: Connectivity and inter-annual variability in the recruitment patterns of European anchovy in the northwestern Mediterranean. *Progress in Oceanography*, *138*, 431–444. https://doi.org/10.1016/j.pocean.2015.01.011

Pepin, P., & Marshall, C. T. (2015). Reconsidering the impossible linking environmental drivers to growth, mortality, and recruitment to fish. *Canadian Journal of Fisheries and Aquatic Science*, *72*, 1–11.

Petrik, C. M., Ji, R., & Davis, C. S. (2014). Interannual differences in larval haddock survival: Hypothesis testing with a 3D biophysical model of Georges Bank. *Fisheries Ocenanography*, *23*, 521–553. https://doi.org/10.1111/fog.12087

Politikos, D. V., Huret, M., & Petitgas, P. (2015). A coupled movement and bioenergetics model to explore the spawning migration of anchovy in the Bay of Biscay. *Ecological Modelling*, *313*, 212–222. https://doi.org/10.1016/j.ecolmodel.2015.06.036

Pritt, J. J., Roseman, E. F., & O'Brien, T. P. (2014). Mechanisms driving recruitment variability in fish: Comparisons between the Laurentian Great Lakes and marine systems. *ICES Journal of Marine Science*, *71*, 2252–2267. https://doi.org/10.1093/icesjms/fsu080

Rose, K. A., Fiechter, J., Curchitser, E. N., Hedstrom, K., Bernal, M., Creekmore, S., … Agostini, V. (2015). Demonstration of a fully-coupled end-to-end model for small pelagic fish using sardine and anchovy in the California Current. *Progress in Oceanography*, *138*, 348–380. https://doi.org/10.1016/j.pocean.2015.01.012

Rykaczewski, R., & Checkley, D. M. Jr (2008). Influence of ocean winds on the pelagic ecosystem in the upwelling areas. *Proceedings of the National Academy of Sciences*, *105*, 1965–1970. https://doi.org/10.1073/pnas.0711777105

Scheffer, M., Baveco, J. M., DeAngelis, D. L., Rose, K. A., & van Nes, E. H. (1995). Super- individuals a simple solution for modelling large populations on an individual basis. *Ecological Modelling*, *80*, 161–170. https://doi.org/10.1016/0304-3800(94)00055-M

Shchepetkin, A. F., & McWilliams, J. C. (2005). The regional oceanic modeling system (ROMS): A split-explicit, free-surface, topography-following-coordinate oceanic model. *Ocean Modelling*, *9*, 347–404. https://doi.org/10.1016/j.ocemod.2004.08.002

Siddon, E. C., Kristiansen, T., Mueter, F. J., Holsman, K. K., Heintz, R. A., & Farley, E. V. (2013). Spatial mismatch between juvenile fish and prey provided a mechanism for recruitment variability across contrasting climate conditions in the eastern Bering Sea. *PLoS ONE*, *8*, e84526. https://doi.org/10.1371/journal.pone.0084526. Pmid: 24391963

Song, H., Miller, A., McClatchie, S., Weber, E., Nieto, K., & Checkley, D. M.. Jr (2012). Application of a data-assimilation model to variability of Pacific sardine spawning and survivor habitats with ENSO in the California Current system. *Journal of Geophysical Research: Oceans*, *117*, C03009.

Watkins, K. S., & Rose, K. A. (2013). Evaluating the performance of individual-based animal movement models in novel environments. *Ecological Modelling*, *250*, 214–234. https://doi.org/10.1016/j.ecolmodel.2012.11.011

Weber, E. D., Chao, Y., Chai, F., & McClatchie, S. (2015). Transport patterns of Pacific sardine *Sardinops sagax* eggs and larvae in the California Current System. *Deep-Sea Research I*, *100*, 127–139. https://doi.org/10.1016/j.dsr.2015.02.012

Xu, Y., Chai, F., Rose, K. A., Niquen, M. C., & Chavez, F. P. (2013). Environmental influences on the interannual variation and spatial distribution of Peruvian anchovy (*Engraulis ringens*) population dynamics from 1991 to 2007: A three-dimensional modelling study. *Ecological Modelling*, *264*, 64–82. https://doi.org/10.1016/j.ecolmodel.2013.01.009

Zajac, Z., Stith, B., Bowling, A. C., Langtimm, C. A., & Swain, E. D. (2015). Evaluation of habitat suitability index models by global sensitivity and uncertainty analyses: A case study for submerged aquatic vegetation.

Ecology and Evolution, *5*, 2503–2517. https://doi.org/10.1002/ece3.1520

Zwolinski, J. P., & Demer, D. A. (2013). Environmental and parental control of Pacific sardine (*Sardinops sagax*) recruitment. *ICES Journal of Marine Science*, *71*, 2198–2207.

Zwolinski, J., Emmett, R., & Demer, D. (2011). Predicting habitat to optimize sampling of Pacific sardine (*Sardinops sagax*). *ICES Journal of Marine Science*, *68*, 867–879. https://doi.org/10.1093/icesjms/fsr038

How to cite this article: Politikos DV, Curchitser EN, Rose KA, Checkley DM Jr, Fiechter J. Climate variability and sardine recruitment in the California Current: A mechanistic analysis of an ecosystem model. *Fish Oceanogr*. 2018;27:602–622. https://doi.org/10.1111/fog.12381